Size Sorting of Fine Grained Sediments During Erosion

by

Brent A. Law

Submitted in partial fulfilment of the requirements
for the degree of Master of Science

at

Dalhousie University
Halifax, Nova Scotia
March, 2008

Library and
Archives Canada

Published Heritage
Branch

395 Wellington Street
Ottawa ON K1A 0N4
Canada

Bibliothèque et
Archives Canada

Direction du
Patrimoine de l'édition

395, rue Wellington
Ottawa ON K1A 0N4
Canada

Canada

DALHOUSIE UNIVERSITY

This thesis is dedicated to my wonderful wife Jennifer and our hilarious son

Zachary who continues to keeps us laughing. Thank-you for everything.

Table of Contents

List of Tables

List of Figures

Abstract

Sediment cores from the western Gulf of Lions, France, were subjected to known bottom shear stresses with the goal of understanding size-specific sediment erodibility. On cruises in October, 2004 and February and April, 2005, cores with an undisturbed sediment-water interface were collected along a transect extending seaward from the mouth of the Tet River. The cores were exposed to increasing shear stresses (0.01 to 0.4 Pa) onboard the vessel shortly after collection by using a Gust microcosm erosion chamber. Samples of the suspensate were collected during the erosion experiments and analyzed for disaggregated inorganic grain size (DIGS) using a Coulter Multisizer IIe. Size-specific relative mobility plots were generated by dividing the proportion of each grain size in suspension at each shear stress by its proportion in the sediment before erosion. If all grain sizes that make up the bottom sediment are eroded equally from the bed, then mobility equals one for all grain sizes. Values > 1 indicate that the suspended sediment is enriched in the size class, and values < 1 indicate that the size class is enriched in the bed. Results show that in non-cohesive, sandy silts, fine grains (clays and fine silts) are eroded preferentially from the bed at low shear stresses. With increasing bottom stress, progressively larger grains are eroded from the bed. In cohesive silts, preferential erosion of the finer sizes no longer occurs, with all sizes up to medium silts eroding at approximately the same rate. Effectively, a sandy silt can be winnowed of its fine grain fraction during erosion, while silts cannot. This difference in the sortability of cohesive and non-cohesive sediment during erosion may control the position and maintenance of the sand-mud transition and the sequestration of surface-adsorbed contaminants.

Acknowledgements

I would like to sincerely thank both Tim Milligan and Paul Hill for getting me stuck in the mud and especially for the fun involved with field studies. Thanks to Kristian Curran for help in the field, sample processing and finishing a few "giraffes". Thanks to Pat Wiberg and Rob Wheatcroft for help in the field and with earlier drafts of the manuscript that led to this thesis. Thanks to my committee members, Alex Hay, Markus Kienast, and Larry Sanford for their insight and suggestions. Finally, thanks are given to all members of the EuroSTRATAFORM cruises in the Gulf of Lions and the after math at the Café de "Rance".

Chapter 1

Introduction

1.1 Background

Erosion and transport dynamics of cohesive sediments are important to many

disciplines, yet understanding of these processes is incomplete (Black et al., 2002). Data

on cohesive sediment resuspension and transport are needed by engineers to solve

problems associated with water quality, navigation, and shoreline stability. Modellers

also need data to calibrate key model parameters and to validate predictions (e.g., Black

et al., 2002, Stevens et al., 2007). Most of the research on the resuspension of cohesive

sediments has focused on bulk erosion rates and cumulative mass eroded under different

stresses (e.g., Sanford and Maa, 2001, Stevens et al., 2007). Little effort has been

directed towards measuring size-specific erosion rates. This observation gap is important

to fill for several reasons. Small particles (i.e. clays and fine silts) eroded from the

seabed attenuate more light per unit of mass than larger particles (i.e. coarse silts and

sands) (Sheldon et al., 1972, Boss et al., 2001). They also have more surface area per

unit of mass, so contaminants adsorb preferentially to them (Zwolsman et al., 1996,

Milligan and Loring, 1997). As well, size distributions in fine sediments are becoming

increasingly useful as a proxy for paleocurrent intensity (McCave et al., 2006). For these

reasons, understanding of the size sorting of fine sediments during erosion is vital.

In the ocean, boundary shear stress is defined as the force per unit of area that flowing water exerts on the seabed. Wiberg and Smith (1987) state that particles at the surface of the seabed will move when the downstream (i.e. fluid drag) and upward (i.e. fluid lift) forces overcome the forces keeping a particle in contact with the bed (i.e. gravity). Bed sediments begin to move when the stress on the bed reaches a critical erosion shear stress, denoted τ_c (Einstein, 1950, Partheniades, 1962, Amos et al., 1992, Tolhurst et al., 1999).

The dominant factors causing the erosion of the seabed are waves and currents, whereas particle size, cohesiveness, water content, and stickiness due to biological activity control erosion resistance (Maa et al., 1998, Sanford and Maa, 2001). The importance of the physical properties of sediments, such as grain size, porosity, and cohesion, on erodibility has long been recognized (Hjulstrom, 1939, Postma, 1967). However, the overall understanding of cohesive sediment resuspension is incomplete because it is governed by not only hydrodynamic forces and the force of gravity, like non-cohesive sediment resuspension, but it is also greatly affected by cohesion, which depends on biological and electrochemical variables (Black et al., 2002).

Historically there have been many investigations of the erosion of non-cohesive and cohesive seabeds. Examples of non-cohesive sediment erosion include Shields, (1936), and Soulsby (1997). Cohesive erosion studies include those of Winterwerp (1989), Amos et al. (1992) and (1997) just to name a few. In the broadest terms non-cohesive sediments have mean grain sizes >63 μm, and are referred to as "sands". Cohesive sediments or "muds" are dominated by fine grained particles that are <63 μm.

The erosion of sand-mud mixtures, however, is not well understood (van Ledden et al., 2004).

Deposition, transport, and erosion of fine sediments is fundamentally affected by aggregation (McCave, 1984, Kranck and Milligan, 1991). Aggregation is the process whereby particles adhere either by electrochemical attraction or organic bonding, thus forming large porous agglomerations called "aggregates" or "flocs". Aggregates sink much faster than the component particles within them (Sternberg et al., 1999). Therefore, settling within aggregates is responsible for the majority of deposition of fine cohesive sediments (Kranck, 1980, McCave et al., 1995, Curran et al., 2002).

Until recently the effect of aggregation on the erosion of bottom sediments has been poorly known. Thomsen and Gust (2000) used a video camera to record eroding in-situ cores and showed that the resuspension of bottom sediments occurs first as aggregates. This result was later confirmed by Roberts et al. (2003) using a flume capable of eroding sediment cores in-situ. The applied bottom shear stress and the sediment texture (i.e. muddy, presumably cohesive, versus sandy, presumably non-cohesive) determined if eroded aggregates persisted and if transport occurred primarily in suspension or as bedload. Roberts et al. (2003) showed that muddy, cohesive sediments were eroded and transported as suspended and bedload aggregates, whereas, sandier, non-cohesive sediments were eroded as aggregates which then broke up to be transported as single grains, predominantly as bedload. While these studies defined broadly the mode of erosion and transport, they did not elucidate the degree of size sorting that occurred.

Despite the importance of aggregation to particle transport and deposition, understanding of the extent of flocculation in the water column and in sediment deposited

3

on the seabed has grown only recently. A promising tool in the understanding of the deposition and transport of fine grain cohesive sediments is the analysis of disaggregated inorganic grain size (DIGS) distributions (Kranck and Milligan, 1991, Curran et al., 2002, Fox et al., 2004, Milligan et al., 2007). A DIGS sample is one in which all organics have been removed, and any bonds between the remaining inorganic component grains have been disrupted. In general, this method relies on the assumption that flocs incorporate into their structure all fine sediment sizes in an unbiased way (Kranck, 1980). Loss of flocs from a parent population either in suspension or resuspended from the seabed does not alter the overall size distribution of the remaining population. Single-grain transport, however, does sort particles according to size, thereby producing evolution in the size distribution of the remaining population (Kranck et al., 1996).

1.2 Goal and Objectives

The goal of this study is to develop greater understanding of the erodibility of fine grained sediment and its role in the generation of sedimentary facies on the continental shelf. In particular, it focuses on the role of boundary shear stress in determining bottom sediment size and sorting during erosion.

The proposed research has three primary objectives:

- To measure the size-dependent removal of sediment from seabed cores as they are exposed to increasing shear stress;

- To conduct these measurements on cores with a range of sediment textures;

- To compare observed sorting under increasing shear stress to model predictions derived from the literature.

4

Chapter 2

Methods

2.1 Overview

As part of the US Office of Naval Research EuroSTRATAFORM program to study processes affecting the transport and accumulation of sediment on continental margins, three sampling cruises took place on the Tet margin, Gulf of Lions, France. The cruises were during October, 2004 and February and April, 2005. The Gulf of Lions, located in the north-west Mediterranean Sea, is a continental margin with a narrow crescent-shaped continental shelf (70 km wide) (Fig.2.1). The Rhone River accounts for up to 80% of the suspended sediment (6-10 x 10^9 kg / yr) delivered to the Gulf of Lions. Sediment from the Rhone is transported along the margin to the southwest, with a significant portion moving offshore through a network of submarine canyons. This study was conducted offshore of the Tet River, which delivers ~6 x 10^7 kg sediment per year with the majority of its yearly sediment load being delivered during floods.

A transect located directly off the mouth of the Tet River was sampled extensively for sediment cores and near bottom water (Fig 2.1). Seabed samples were collected using a slo-corer, which is a hydraulically-damped gravity corer that preserves the sediment-water interface during sampling. It uses a 350-kg lead weight and a
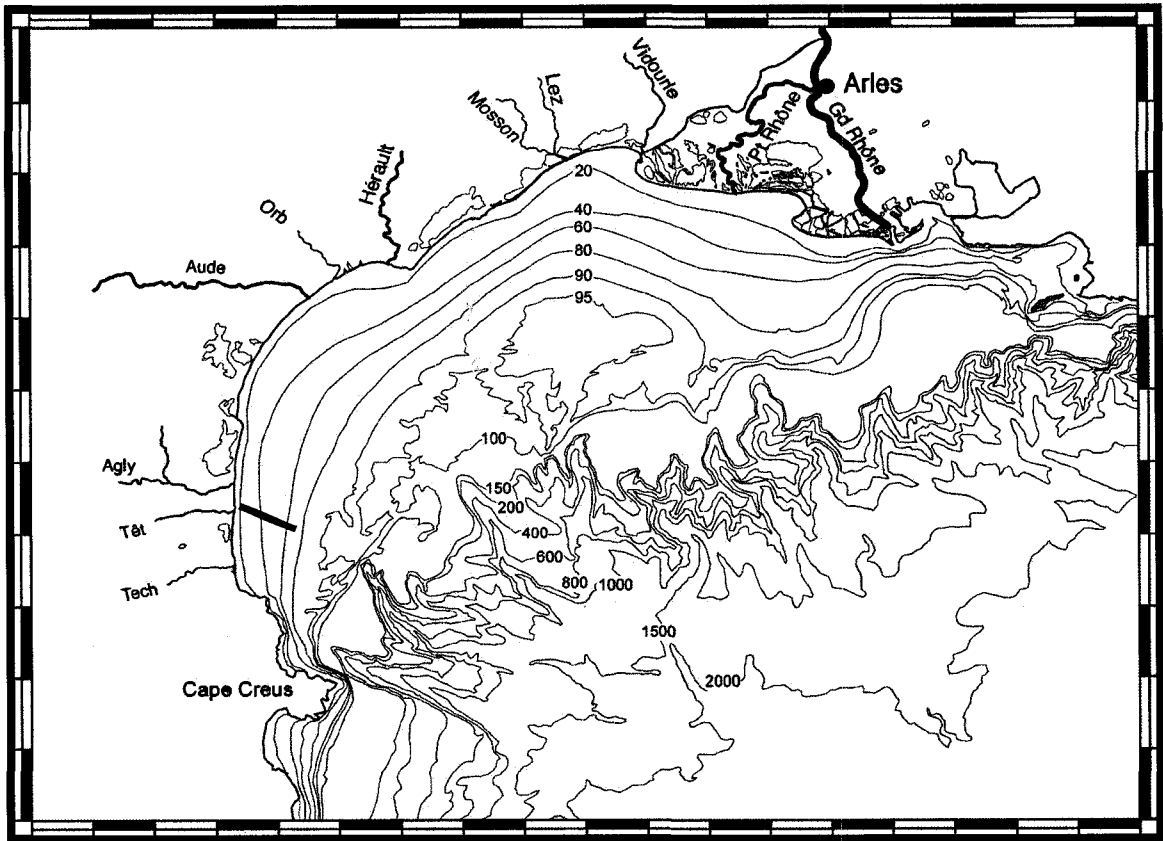
Fig 2.1. A plot of the study area in the Gulf of Lions, France. The Tet River transect is marked with a black line and is labelled on the map. A transect of stations directly off the mouth at 20, 28, 35, 40, 45, 56, and 74 meters water depth were extensively sampled to collect bottom cores and near bottom water samples for erosion experiments. Contour lines on the map represent water depth in meters.

hydraulically damped plunger to push a 10.8-cm diameter polycarbonate core barrel into the bottom sediment (Fig 2.2). Up to six replicate cores were taken at each station. In October 2004, two cores from each station were used to determine erosion thresholds and the evolution of particle size in suspension. Three cores were used during the two cruises in 2005. Erosion thresholds were determined using a Gust chamber (Gust and Muller, 1997, Tolhurst et al., 2000). The evolution of grain size was determined using an electoresistance particle size analyzer (Coulter Counter). The other cores were used to measure replicate, high-resolution porosity profiles (based on microresistivity profiling, Wheatcroft, 2002) and to determine the particle size (i.e. DIGS) of an uneroded surface. At each station a CTD profile was taken and a rossette sampler was used to collect near-bottom water for use in the erosion experiments.

2.2 Gust Chamber

The Gust chamber is a circular erosion device that comprises a housing with a rotating shear plate, a removable lid, and water input and output connections. It fits directly onto a slo-core tube (Fig 2.3 and 2.4). By controlling both the rotation rate of the shear plate and the rate at which water is pumped through the device, a uniform shear stress can be applied across the sediment surface. Calibration equations relating shear velocity to shear stress were obtained from the calibrations carried out by G. Gust (Gust and Muller, 1997). Using hot-film sensors flush mounted to the seabed to record bottom stress, the required pumping rate and rotation of the stirring disk were adjusted to obtain homogenous shear stress across the sediment surface. The hot-film probes maintain a
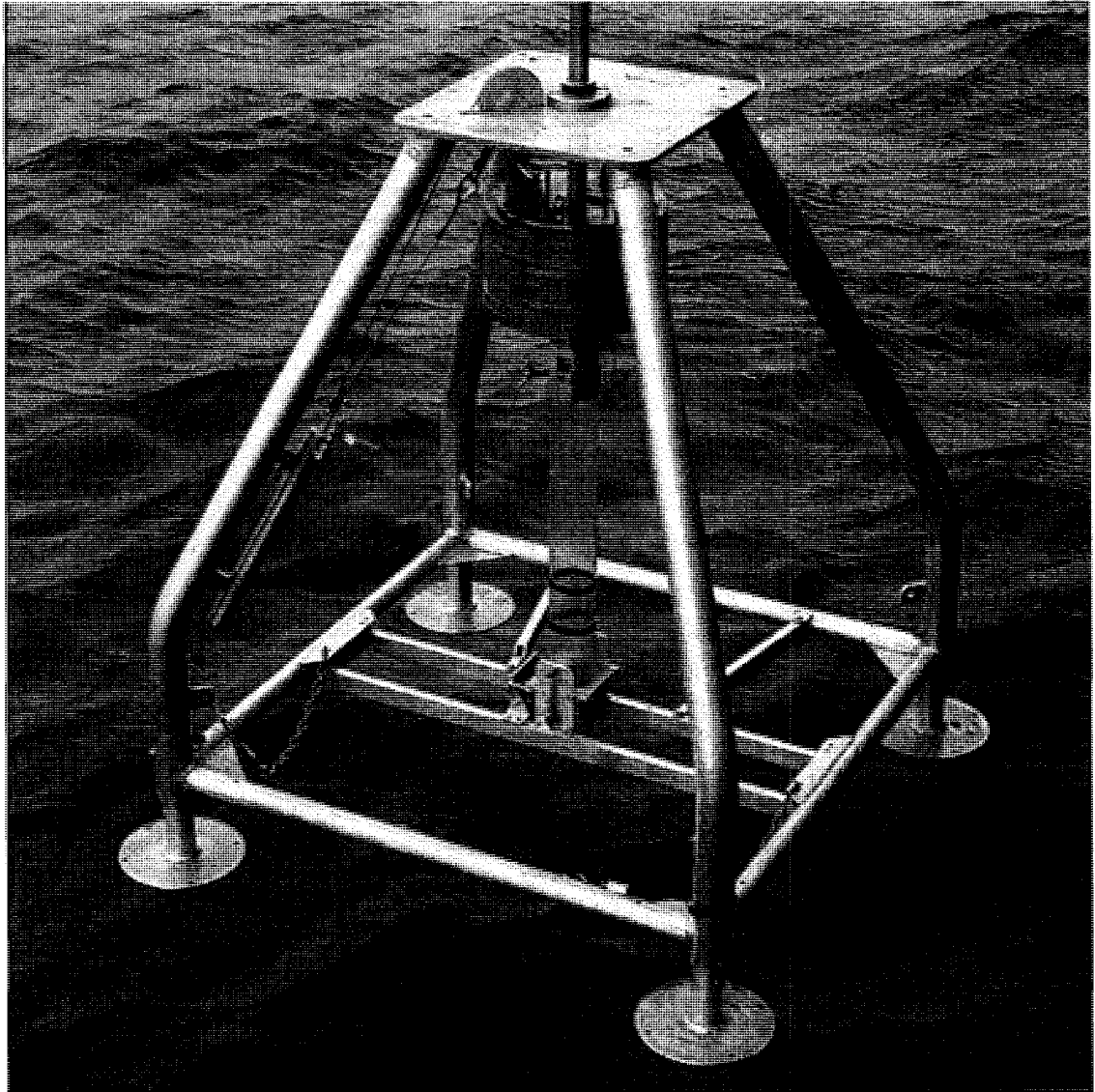
Fig 2.2. A photo of the hydraulically damped slo-corer.

Gust Chamber   **Turbidity meter**   **Pump**   **Laptop**
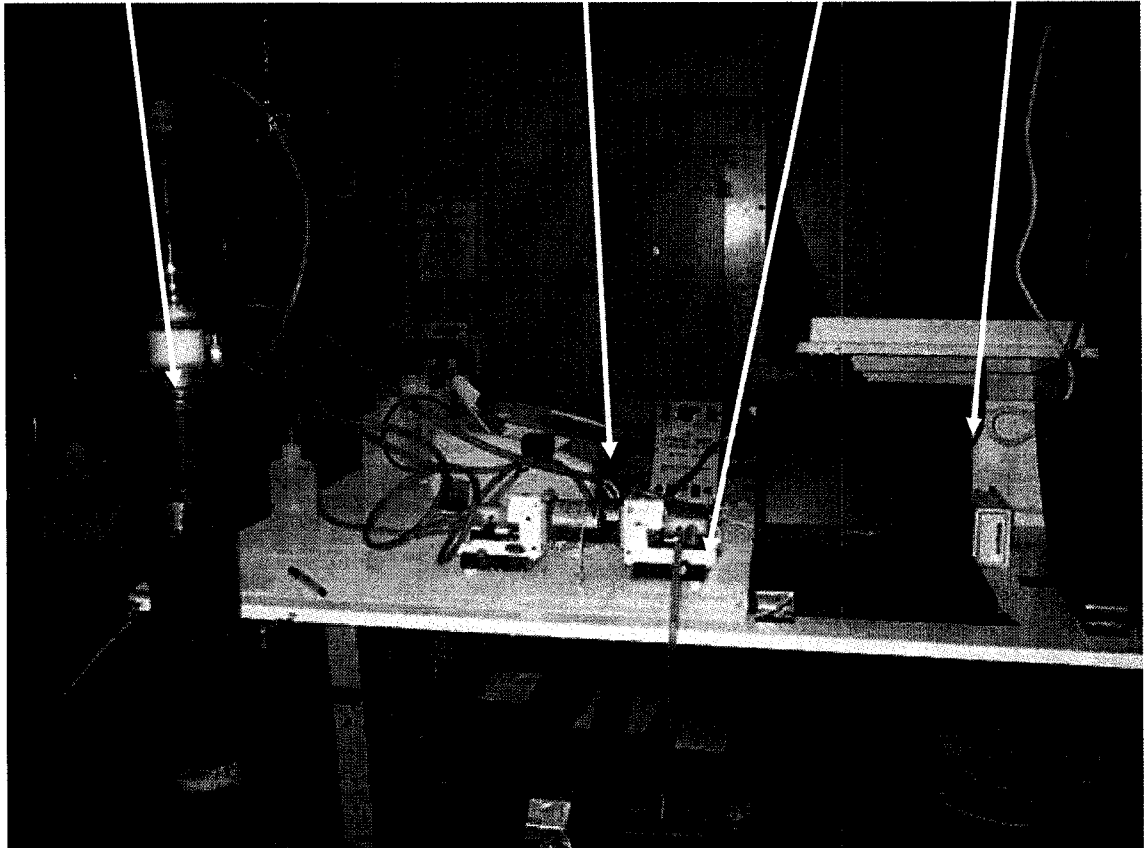
Fig 2.3. A photo of the Gust Chamber and equipment used for erosion studies.
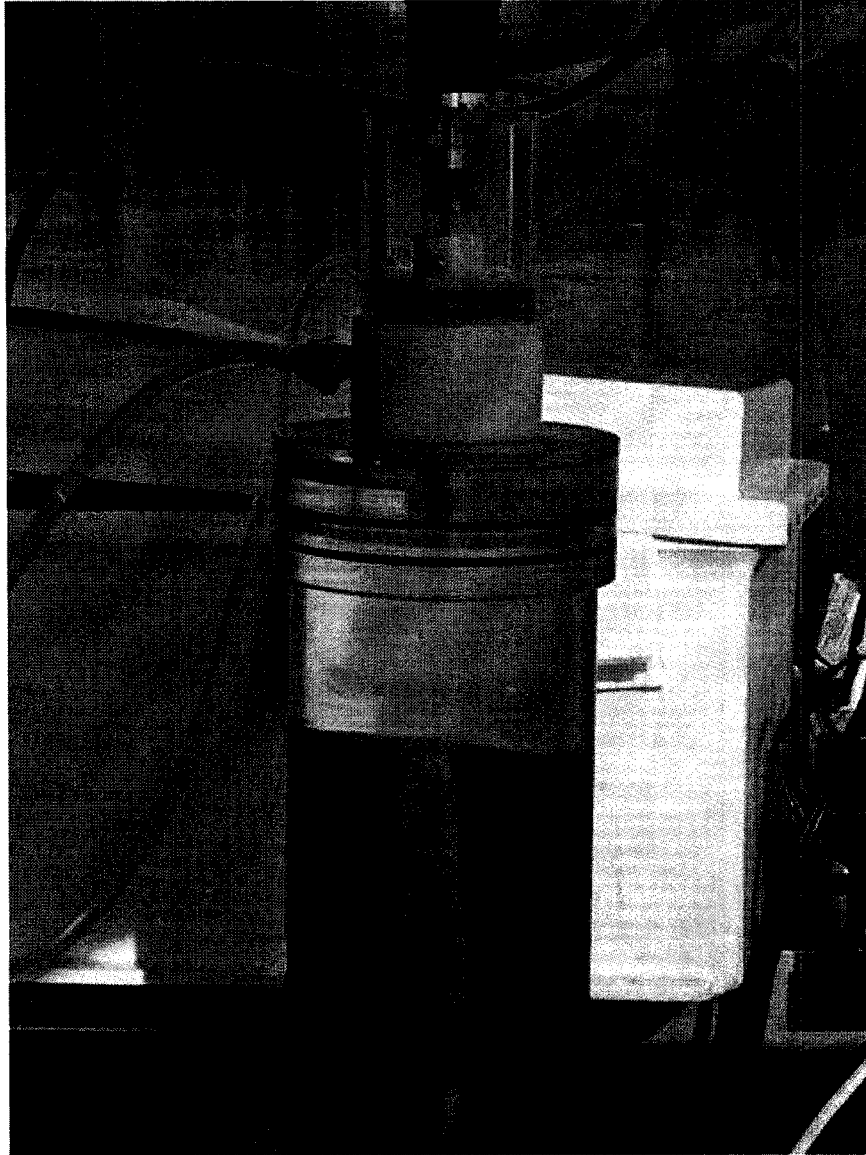
Fig 2.4. A photo of the Gust microcosm erosion device used to erode the tops of collected cores under increasing shear stress steps of 0.01, 0.08, 0.16, 0.24, 0.32, and 0.40 Pascals (Pa). The suspensate collected was filtered for SPM to calculate erosion rates and for grain size analysis (DIGS) on a Coulter Multisizer IIe.

constant temperature. As the spinning rate of the disk increases, the thermal boundary layer near the sensors compresses, resulting in greater heat flux away from the probe. A voltage increase is needed to maintain a constant temperature. The faster the flow, the higher the voltage required. Calibrations performed by Gust were also carried out using sediments with independently measured critical erosion shear stresses, primarily kaolinite.

In cohesive sediments, critical erosion shear stress tends to increase with depth below the seabed (Amos et al., 1992). This tendency arises due to compaction and associated increased contact area among cohesive sediment grains. As a result, a fixed amount of sediment is available for erosion from the seabed at a given shear stress and the bed erodes downward until the critical shear stress of the sediment becomes larger than the applied stress. Therefore, as suspensate with eroded bed sediment is replaced with background water, turbidity of the suspensate falls and eventually returns to background values. Background water was collected using a CTD Rosette one meter off the bottom at each sampling site. Turbidity of the suspensate was measured using a Hach 2100 Laboratory Flow through turbidity meter. The time to return to background turbidity levels was generally around 20 minutes for each shear stress step. Shear stresses applied to cores for this study were 0.01, 0.08, 0.16, 0.24, 0.32, and 0.40Pa, with the first step of 0.01Pa being used to flush the tubing. The water pumped from the Gust chamber was collected in a 2-L flask and filtered for suspended particulate matter (SPM) and particle size analysis. The SPM data was used to determine the mass of sediment eroded at each shear stress and to calibrate continuous turbidity measurements made with a flow-through turbidity meter. The focus of this study was the size distribution of the

collected suspended sediment samples and how it compared to the size distribution of the underlying bed sediments. For a full description of the Gust microcosm erosion device, its function, and calibration, see Gust and Muller (1997) and Tolhurst et al. (2000).

2.3.1 Particle Size

The disaggregated inorganic grain size (DIGS) distributions of the suspended sediment and the bottom core samples were determined using a Coulter Counter Multisizer IIe (Fig 2.5). Particle sizes are binned in 1/5 phi intervals (ϕ = $-\log_2 d$ (d= diameter in mm)). Three tubes with a 30, 200 and 400μm diameter aperture were used to obtain the DIGS distribution. With this configuration the Coulter Counter measured volume concentration in size bins covering a diameter range of 0.8 to 260μm. Suspended sediment samples were analyzed for all shear stress steps at each station occupied on the Tet transect. Surficial bottom samples from the tops of cores both before and after erosion experiments were analyzed to determine the change in bed grain size after each erosion experiment. For the uneroded cores the top 0.5cm was sampled to be consistent with the predicted depth of erosion by the Gust chamber.

2.3.2 Suspended Sediment DIGS Analysis

To determine the total suspended particulate matter (SPM), known volumes of water were filtered onto Millipore 8.0μm SCWP (cellulose acetate) pre-weighed filters using standard gravimetric methods. Millipore filters were selected because they have much lower effective pore sizes than indicated once filtering begins, and they have
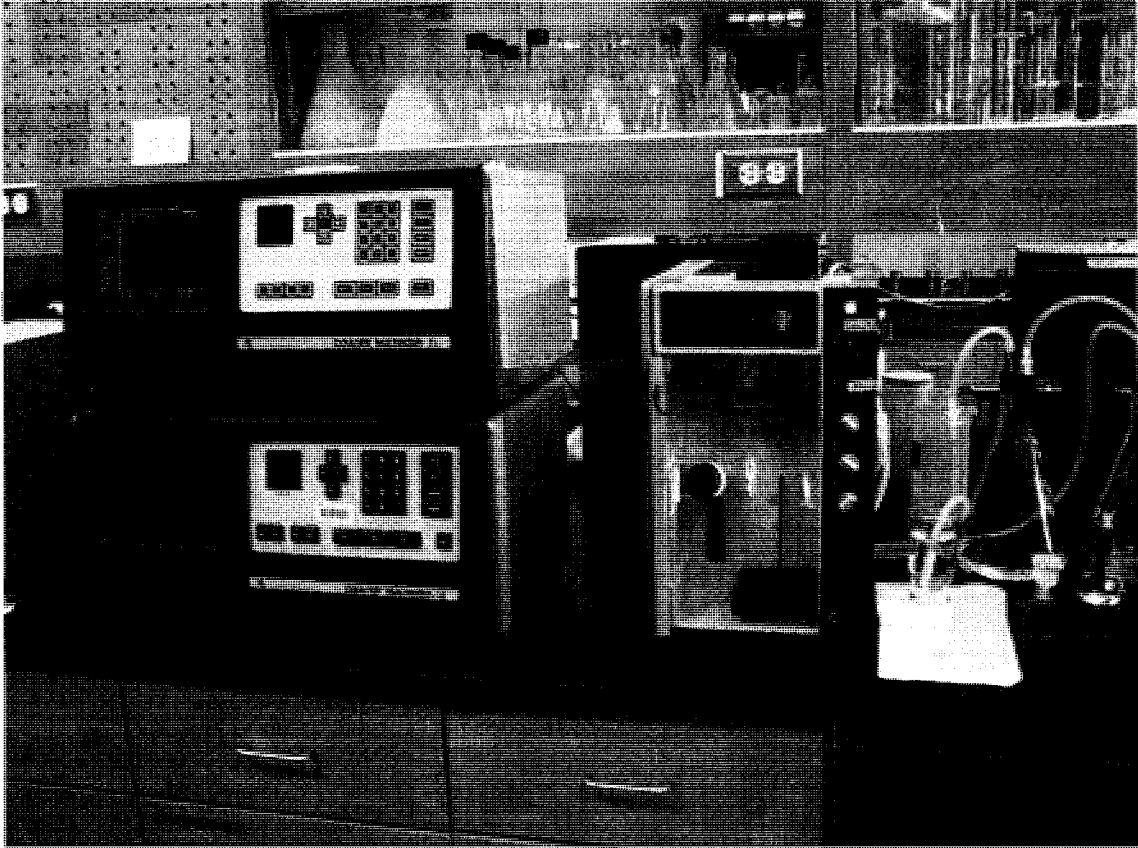
Fig 2.5. A photo of a Coulter Counter Multisizer IIe, the electroresistance particle size analyzer used for DIGS analysis.

excellent trapping efficiency (Sheldon, 1972). The filters were dried at < 60°C and weighed to obtain a sediment mass and to determine SPM concentration. For DIGS analysis samples were placed in a low temperature (<60°C) oxygen-plasma asher to remove the filter and organic matter and to prevent the fusing together of mineral grains. Once removed from the asher, samples were treated with hydrogen peroxide 35% (H_2O_2) to remove all remaining organic residue, so only inorganic grains remain. Inorganic suspended sediments were resuspended in a 1% NaCl electrolytic solution and disaggregated with a sapphire-tipped ultrasonic probe prior to analysis on the Multisizer. The Multisizer IIe draws the resuspended solution through an aperture of known diameter using a vacuum. The vacuum pressure is set to 150 mm/Hg. As particles pass through the aperture sensing zone, the change in the electrical impedance between an electrode inside the aperture tube and an external electrode produces a voltage peak that is proportional to particle volume. The voltage peaks are counted and associated with an equivalent spherical diameter (esd), based on calibration of aperture tubes using particles of known diameter and volume. Once a sample is analyzed, data from the Coulter Counter is streamed via an RS-232 cable to a computer running DOS software that was written in the Particle Dynamics Lab at Bedford Institute of Oceanography. The software, called "MEDIT" (for Multisizer Edit) plots the volume concentration versus diameter data on log-log plots. The concentration of particles in overlapping channels from two tubes should be equal, but in practice they must be aligned with MEDIT to form a smoothed histogram for the entire grain size spectra. The suspended sediment DIGS are expressed as volume concentration in parts per million (ppm) and plotted as log concentration vs. log diameter in micrometers.

2.3.3 Bottom Sediment DIGS Analysis

Organic matter was removed from bottom sediments with 35 % hydrogen

peroxide (H_2O_2). Bottom sediments were also resuspended in 1% NaCl electrolytic

solution and the process of running samples on the Coulter Counter was the same as with

the suspended sediments. The DIGS of bottom sediments obtained from the Multisizer

are expressed as log of equivalent volume fraction, which is equivalent to mass fraction

assuming a constant particle density of 2650 kg/m^3, vs. log of the diameter. According to

the Coulter manual, relative error in concentration in a given channel is < 10%.

Reference materials or duplicate samples run in the Particle Dynamics Lab up to several

years apart show relative errors in a given size class generally << 10%. For a complete

description of the methods of the particle size analysis used herein see Kranck and

Milligan (1979) and Milligan and Kranck (1991).

2.4 Determination of Size- Specific Relative Mobility

Size-specific relative mobility (SSRM) is defined as the suspended sediment

volume fraction of a given size interval just above the seabed divided, denoted i_a , by the

volume fraction for the same size interval in the seabed, denoted i_b. To quantify the

SSRM, the volume fraction of each size class of sediment suspended by the Gust

chamber for each bottom stress was divided by the corresponding volume fraction from

the top of an uneroded core at the same station:

$$SSRM(i) = {i_a}/{i_b}$$

(1)

The seabed volume fractions used in calculations of SSRM represent the average DIGS spectra from the top 0-0.5cm from at least two slo-cores from the same station location. Mobilities equal to unity indicate that the grain sizes that make up the bottom sediment are eroded equally from the bed. Values >1 indicate that the suspended sediment is enriched in the size class relative to the bed sediment, and values < 1 indicate that a size class is more common in the bed than in suspension.

When calculating mobilities, background volume concentration above the bed was subtracted for each station at every shear stress level. Bottom water that was collected 1m off the bed using a CTD rosette was filtered and analyzed for DIGS. This same water was pumped into the Gust chamber during erosion studies, and is considered to be the background suspended sediment concentration for each sampling station. The background size distribution (i.e. DIGS) was subtracted from all size distributions obtained from suspension. When calculating theoretical mobilities model parameters such as the density and viscosity of seawater are a function of the temperature and salinity of the background water at the time of sampling.

Chapter 3

Results

The bottom sediments on the Tet transect are of mixed grain size composed primarily of muds (<63um mean diameter). Inner-shelf samples from 15m to 45m depth have decreasing percentages of fine sand from 33% to 10%. The stations on the outer shelf beyond the 45m isobath contain sand fractions between 2%-6% (Fig. 3.1; Table 3.1).

The across-shelf DIGS spectra (Fig. 3.1) show a change in shape from station T35 to T45. Station T35 shows a DIGS distribution with a coarse silt mode and a relatively minor fine silt and clay tail. The bed sediment at T45 has a larger percentage of fine sediment and lacks the distinct coarse silt mode. The greatest changes in median diameter and in the <16μm fraction derived from DIGS spectra occur between the 35 and 45 meter isobaths.

Size-specific mobilities on the Tet transect change progressively from the inner-shelf sediments, past the grain-size transition, and into the deeper water of the outer shelf. Fine silts and clays in inner-shelf sediments (e.g., stations T20, T28, T35) have high
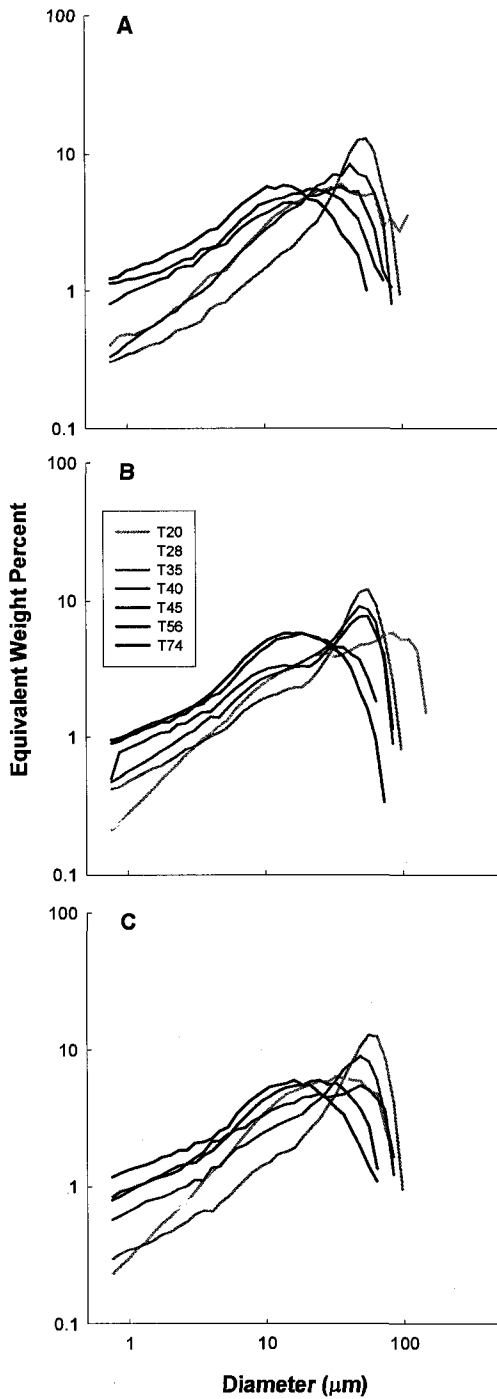
Fig 3.1. A plot of the across shelf grain size collected at stations along the Tet transect during the (A) October 2004, (B) February, and (C) April, 2005 cruise. The DIGS distributions represent an average of at least two grain size curves from uneroded core surfaces from the same station location. Maximum expected relative error in DIGS in a given channel is assumed to be < 10%. Between station T35 and T45, size distributions with a distinct coarse silt mode give way seaward to size distributions with mass distributed more evenly among the silts and clays.

18

Oct-04	d50 (µm)	% < 4µm	% < 16µm	% < 63µm	% > 63µm	van Ledden Class
T20	24.3	9.07	35.2	82.4	17.6	VI
T28	38.2	5.57	20.1	82.9	17.1	V
T35	39.9	5.90	19.3	79.7	20.3	V
T40	25.3	8.36	33.1	90.7	9.31	VI
T45	16.3	16.5	49.5	94.7	5.26	VI
T56	13.3	19.1	56.8	97.3	2.71	VI
T74	9.72	23.6	70.7	100.0	0.00	VI
Feb-05	d50 (µm)	% < 4µm	% < 16µm	% < 63µm	% > 63µm	
T20	33.2	7.12	29.4	67.1	32.9	V
T28	43.4	4.52	16.9	75.8	24.2	V
T35	37.5	8.61	25.9	81.4	18.6	VI
T40	26.9	10.8	35.1	88.5	11.5	VI
T45	22.7	13.9	41.5	89	11	VI
T56	13.5	17.1	56.7	98.2	1.8	VI
T74	12.2	17.9	61.5	93.6	6.4	VI
Apr-05	d50 (µm)	% < 4µm	% < 16µm	% < 63µm	% > 63µm	
T20	21.1	7.99	39.2	91.1	8.9	VI
T28	32.0	8.25	30.8	81.3	18.7	VI
T35	42.2	6.04	19.4	73.9	26.1	V
T40	27.8	11.3	34.5	89.1	10.9	VI
T45	21.0	16.7	47.9	90.9	9.1	VI
T56	14.4	16.1	54.5	98.7	1.3	VI
T74	11.2	21.6	65.8	98.9	1.1	VI

Table 3.1. The physical characteristics of bottom sediments from the October, 2004, February, and April, 2005 sampling along the Tet transect. Values of d50 (median diameter), %<4um, %<16um, %<63um, and, %>63um are average values from the top of all non-eroded cores. The last column represents the classification of sediment based on van Ledden et al., (2004). It uses a sand-silt-clay ternary diagram to identify six categories of sediment based on whether the sediment matrix was supported by sand, silt, or clay and whether the sediment was cohesive or non-cohesive. It uses a threshold of 7.5% clay (i.e. < 4µm) to distinguish cohesive and non-cohesive mixtures (see discussion).

mobilities at low shear stress (Fig 3.2). In other words, sediments suspended at low shear stresses are enriched in fines in comparison to the bed. As stress increases larger grains are eroded and mobilities approach values near unity at the maximum applied stress of 0.4 Pa. Near the grain-size transition at station T40, mobility values are >1 but < 10, and fine sand grains are not eroded from the seabed (Fig 3.2). At Station T56 and T74 mobilities are close to unity for all but the coarsest grain sizes for all increasing shear stress steps, indicating that individual grain size classes are being eroded in proportions equal to the seabed (Fig 3.2).

Compared to the October 2004 and February 2005 data, mobility plots from April for the inner-shelf stations show decreases in the mobilities of finer grain sizes at lower stresses (Fig 3.3). This decrease is associated with an increase in the relative proportion of fine silt and clay in the seabed (Table 3.1). The cause of the finer texture is unknown, but could be due either to accumulation of fines during the late winter and early spring or to spatial variability in texture. Stations at or near the grain-size transition (T40) and seaward showed little or no change in mobility from October, 2004 through February and April, 2005, with values close to unity for all individual grain size classes eroded (Fig 3.3).

(A) DIGS Spectra   **(B) SSRM(i)**

Equivalent Weight Percent

SSRM (i)

T28F Feb   T28C Feb   T28F Feb   T28C Feb

T40B Feb   T40G Feb   T40B Feb   T40G Feb

T56F Feb   T56A Feb   T56B Feb   T56A Feb

0.08Pa
0.16Pa
0.24Pa
0.32Pa
0.40Pa
B Sed

Diameter (µm)   Diameter (µm)
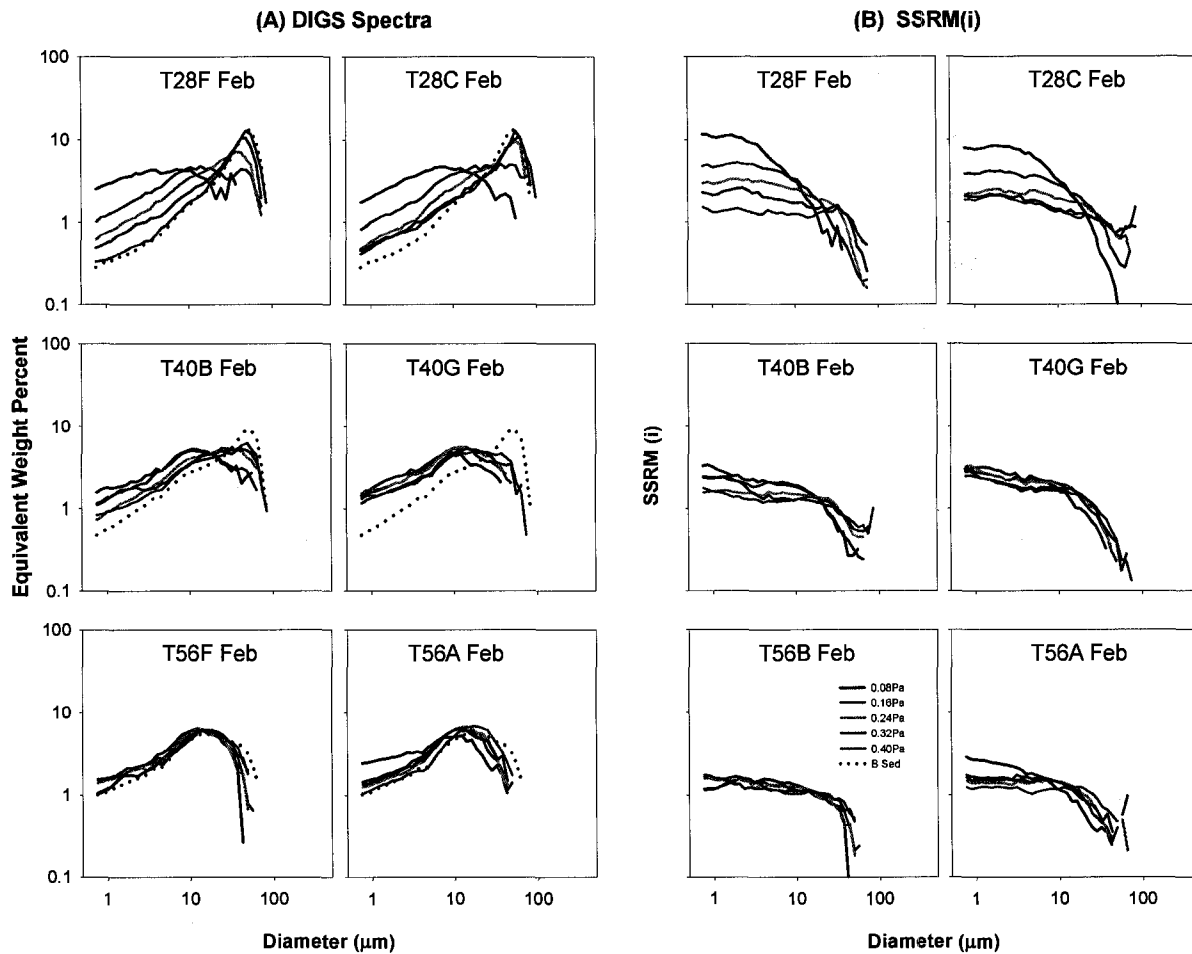
Fig 3.2A. A plot of replicate DIGS spectra for stations T28, T40, and T56 during the February 2005 study. The black dotted line represents the average DIGS of the bottom sediment from the top <0.5cm of cores, and the other 5 colored lines represent the suspended DIGS from increasing bottom shear stress generated from the Gust chamber. 3.2B. SSRM(i) for increasing shear stress steps. At Station T28 fine sediment is enriched in suspension relative to the seabed when applied stresses are low. As stress increases, progressively larger grain sizes are eroded, so mobilities fall for the finer sizes and increase for the larger sizes. As the mud fraction increases moving from station T40 to T56, the preferential erosion of fine sediments at low shear stresses no longer occurs. Instead mobilities are similar for all but the largest grain sizes for all shear stress increments.

T28 Oct <4um = 5.5%

T28 Feb <4um = 4.5%

T28 Apr <4um = 8.3%

T40 Oct

- 0.08 Pa
- 0.16 Pa
- 0.24 Pa
- 0.32 Pa
- 0.40 Pa

T40 Feb <4um = 10.8%

T40 Apr <4um = 11.4%

T56 Oct <4um = 17.1%

T56 Feb <4um = 17.1%

T56 Apr <4um = 16.1%

SSRM(i)

Diameter (µm)
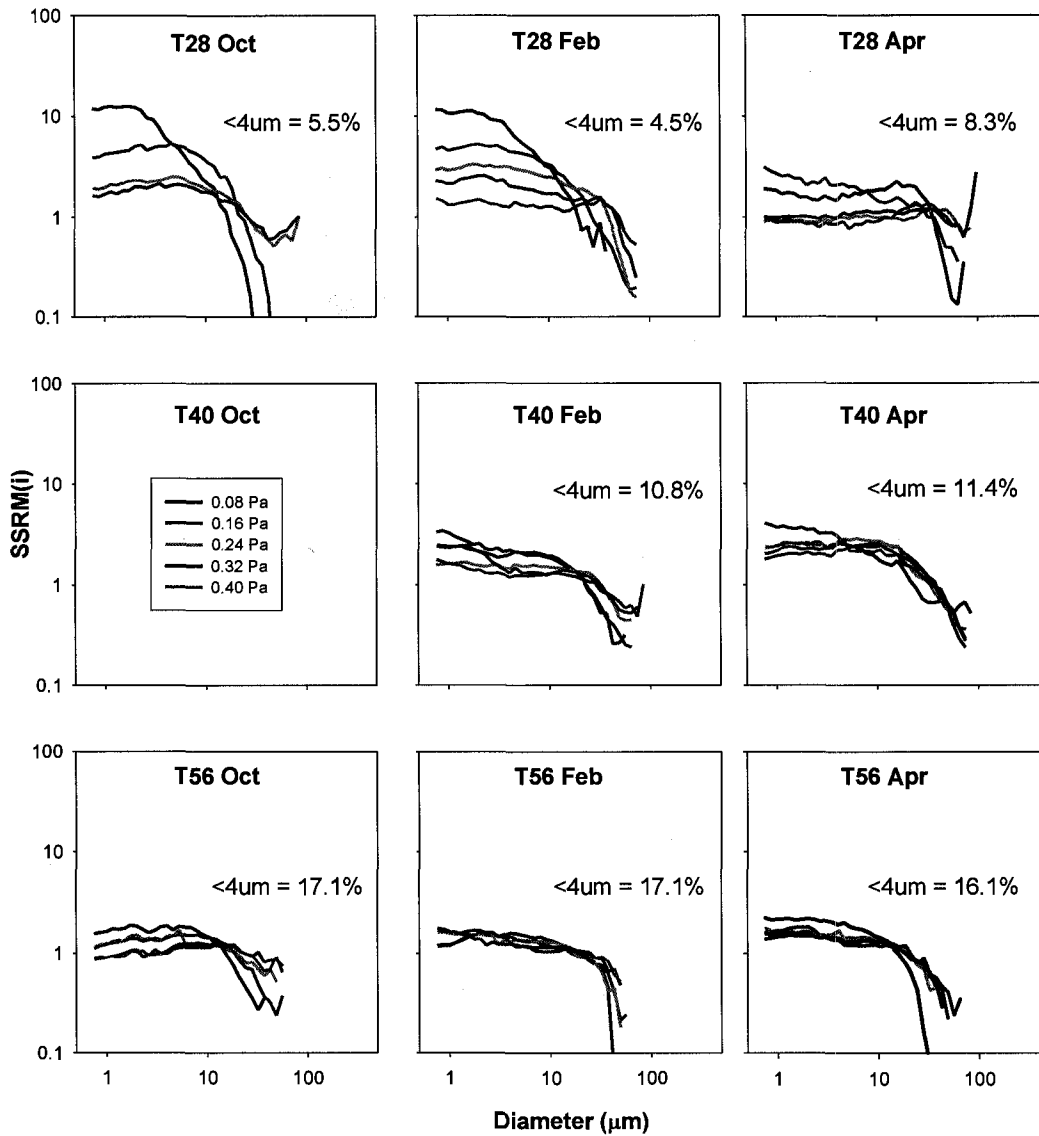
Fig 3.3. A plot of the temporal evolution of mobility over the three study periods. In April at T28, preferential erosion of fine sediment at low shear stress is reduced relative to October and February. An increase in the <4um fraction at station T28 in April accompanies this change, indicating that the fines perhaps act to increase cohesion of the bottom sediment. Sediments from Station T40 have similar mobilities in February and April. No cores were collected there in October. Station T56 has similar mobility over all three study periods.

Chapter 4

Discussion

4.1 Calculation of Theoretical Mobilities

A simplified model is used to calculate theoretical mobilities. The model assumes that for a given excess shear stress, there is a defined reference concentration at a specified reference height above bottom (cf. Smith and McLean, 1977). This approach ignores many potentially important time dependent effects in setting nearbed concentrations within the Gust chamber. It is successful, however, in reproducing the observed mobilities, and therefore is used as a tool for interpreting the observations. A comparison of various model predictions to results yields an understanding of the processes responsible for the different observed responses of mobility to increasing shear stress.

Size-specific relative mobility is equal to the suspended volume fraction just above the seabed divided by volume fraction in the seabed. In the simplified model, the concentration in suspension immediately above the seabed is assumed to equal the reference concentration, Ca_i, which is proportional to the excess boundary shear stress (Smith and McLean, 1977). This concentration is calculated as (Wiberg et al., 1994):

$$Ca_i = i_b x Cb \left(\frac{\gamma S_i}{1 + \gamma S_i} \right) \tag{2}$$

where Ca_i is the concentration of size class i in suspension, i_b is the volume fraction of i in the bed sediment as derived from the normalized seabed DIGS for each station, Cb equals the total volume concentration of bed sediment or (2400 kg/m^3 x (1-porosity), S is excess shear stress $(\tau_b - \tau_c)/(\tau_c)$, and γ is a coefficient of resuspension. A value of 0.001 is used here (Wiberg et al., 1994). Equation 2 can then be used to determine size-specific relative mobility for bottom sediment.

$$\frac{Ca_i}{\sum Ca_i} = \frac{i_b \times Cb\left(\frac{\gamma S_i}{1+\gamma S_i}\right)}{\sum i_b \times Cb\left(\frac{\gamma S_i}{1+\gamma S_i}\right)} = i_a \tag{3}$$

$$\frac{Cb_i}{\sum Cb_i} = i_b \tag{4}$$

$$\frac{i_a}{i_b} = \frac{\frac{(\gamma S_i)}{(1+\gamma S_i)}}{\sum i_b \frac{(\gamma S_i)}{(1+\gamma S_i)}} \tag{5}$$

$$SSRM(i) = \frac{\frac{(\gamma S_i)}{(1+\gamma S_i)}}{\sum i_b \frac{(\gamma S_i)}{(1+\gamma S_i)}} \tag{6}$$

To explore possible controls on observed mobilities, various models that calculate suspended sediment concentration above the seabed are used to predict size-specific relative mobility. Two non-cohesive sediment resuspension models and two cohesive sediment models are implemented. A third cohesive resuspension model is considered based on recent observations of the erodibility of flocs.

24

The first non-cohesive sediment resuspension model explored is that of Wiberg and Smith (1987). This model can be used to calculate the mobility of bottom sediments during resuspension without the effects of bed limitation. This model works with the same principal as Shields (1936) model for eroding individual grains but has better constraints on (τ_c) for small grain diameters. The model can calculate (τ_c) for the erosion of fine grain sizes from both homogeneous (well-sorted) and heterogeneous (mixed) seabeds. For simplicity, the calculations here assume that the bed is homogeneous.

The second non-cohesive resuspension model examined is the model of Wiberg et al. (1994) which introduces an "active layer depth" for erosion. This model was proposed by Wiberg et al. (1994) to reconcile time series of modeled suspended sediment concentration with observed time series of seabed stress and nearbed optical attenuation. The active layer is the layer of bed sediment that is available for resuspension. In non-cohesive sediment, as fine sediment is eroded from the seabed, larger grains now in higher proportion in the seabed armour the bed and protect the remaining finer grain sizes, thereby limiting their availability for resuspension. Similarly, in undisturbed cohesive beds, consolidation of bed sediments increases over time with increasing depth below the sediment-water interface, which limits the supply of sediment available for resuspension at a given shear stress. The active layer depth for our calculations of mobility is set at 1mm, which is an approximation based on the previous erosion studies (Lynn et al., 1990; Wiberg et al., 1994).

Several authors have proposed that in cohesive sediments erodibility is equal for grains smaller than a specified size (Wiberg et al., 1994; McCave et al., 1995). As a

25

corollary, all grains smaller than a specified size share the same critical erosion shear stress. The first cohesive model examined is that of Wiberg et al. (1994). The model uses a critical erosion shear stress of 0.1 Pa to erode all grain sizes < 40μm and suggests that the erosion of the seabed does not occur at lower shear stress due to the cohesive nature of fine particles. The second cohesive resuspension model discussed is that of McCave et al. (1995) which uses 10μm as a discriminator between cohesive and non-cohesive sediments. According to the model of Wiberg and Smith (1987), τ_c for a 10μm silt grain is 0.025Pa, and this value is used to erode all grain sizes <10μm when calculating size specific mobility with this model.

4.2 Model-Data Comparison, Inner (T28) vs. Outer (T56) Shelf

4.2.1 Sediments

Stations T28 and T56 from the Tet transect represent inner-shelf and outer shelf sediments respectively and are compared to models of sediment erosion and transport in the literature as a way to distinguish the erosion behavior and size specific relative mobility of cohesive and non-cohesive sediments. Stations on the inner-shelf (T20, T28, T35) behave non-cohesively with small sediment grains being winnowed from the bed at low shear stresses. Moving past the grain-size transition (T40) and into outer-shelf sediments composed primarily of mud (T56 and T74), sediment grains erode in equal proportion to the sea bed and behave cohesively. In the next section, mobilities from T28 and T56 are compared to the models. The results from these stations are representative of the other stations for both inner and outer shelf sediments.

26

4.2.2 T28

The non-cohesive critical shear stresses of Wiberg and Smith (1987) coupled with Eq. 2 do not explain the mobilities found at station T28 on the Tet transect (Fig. 4.1). The model over-predicts the mobility of fine sediment sizes. It produces high mobilites (>>1) for fine grains and low mobilities (<<1) for larger grain sizes found in the bed sediment (Fig 4.1 a and b) at all shear stresses, which does not match the observed results (Fig 4.1 a and b).

The non-cohesive bed limitation model of Wiberg et al. (1994) predicts mobilites similar to those observed at station T28 and for the stations inshore of the grain-size transition (Fig 4.1 a and c). The mobilities predicted by the model show equal and high mobilities for the finest sizes at low shear stresses. As stress increases, the plateau of equal mobilities for finer sizes decreases and covers a greater range of size classes and increasingly larger grains are resuspended. The equal mobility plateau for the fine diameters occurs for the size classes of sediment that have been completely winnowed from the active layer. At this point, the total mass of small particles in suspension is equal to the mass originally available in the active layer.

Mobilities predicted by the cohesive resuspension models of Wiberg et al. (1994) and McCave et al. (1995) do not resemble the observed mobilities at station T28 (Fig 4.1 a, d, and e). Both models predict equal mobilities for the finest size classes, but they are not high enough at low shear stresses. The plateau over which the mobilities are equal extends over too many size classes, and the plateau of equal mobilities for fine sizes does not decrease with increasing shear stresses.

T28 Feb
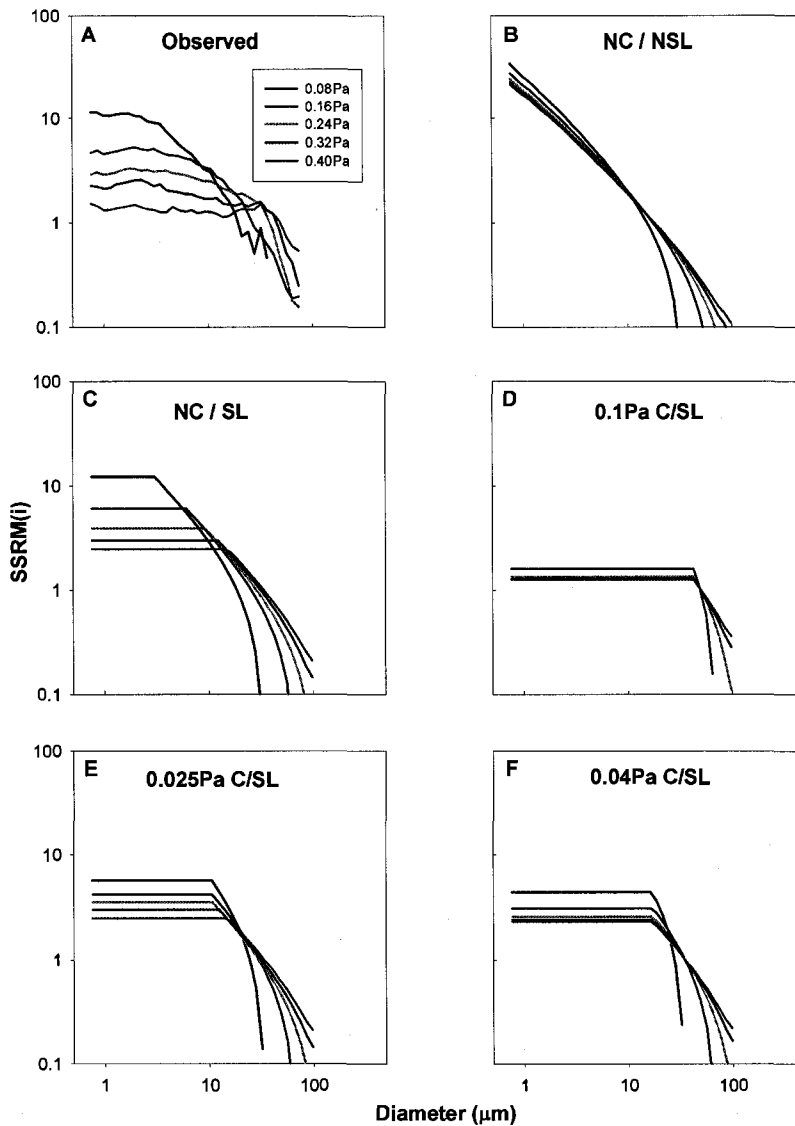
Fig 4.1. Observed and theoretical sediment mobilities for Station T28 in February. Panel (A) shows mobilities generated from the observations. The remaining mobility plots were generated based on theoretical models that exist in the literature for the erosion of cohesive and non-cohesive sediments. Panel (B) shows mobilities for the model that is non-cohesive (NC) and imposes no supply limitation in the seabed (Eq. 1). Panel (C) shows mobilities for the model that is non-cohesive but does impose supply limitation in the bed (also known as bed armoring; Wiberg at al, 1994). Panels (D), (E), and (F) show mobilities for the model that imposes cohesive behavior by assigning a common critical erosion shear stress to all sizes smaller than a specified value. In Panel (D) the limit is 40 μm, corresponding to a critical erosion shear stress of 0.1Pa (Wiberg et al, 1994) for sediment erosion. For Panel (E) the limit is 10 μm, corresponding to a critical erosion shear stress of 0.025 Pa (McCave et al, 1995). In Panel (F) the limit is 16 μm, corresponding to a critical erosion shear stress of 0.04 Pa. All cohesive models also impose supply limitation in the seabed.

28

In summary, at station T28 on the Tet transect the non-cohesive model of Wiberg et al. (1994) works well to predict observed mobilities. This model also predicts observed mobilities for the other inner-shelf sediments. Supply limitation from the bed is needed to limit the amount of erodible fine grain sizes. Cohesion is not needed to reproduce the observed mobilities.

4.2.3 T56

The no-sediment-limitation model (Eq. 1) with critical shear stresses from Wiberg and Smith (1987) does not do well at predicting the mobility of eroded bottom sediments at station T56, which are composed entirely of mud (Fig 4.2 a and b). This model over-predicts the mobility of the small grain sizes. As is the case with the T28 model prediction, this model predicts similar mobilities with increasing shear stress that do not match the observed results.

The Wiberg at al. (1994) non-cohesive supply limitation model does not predict the mobilities seen at station T56 (Fig 4.2 a and c). This model over-predicts the mobility of the smallest grain sizes at low shear stress. It also predicts that the diameter range of equal mobilities for fine size classes grows more with increasing shear stress than is observed.

The cohesive resuspension models of Wiberg et al. (1994) and McCave et al. (1995) both predict trends in mobility for station T56 that resemble observations. Both models predict mobilities that are near unity and equal for a large range of diameters at all shear stresses. Essentially, when muds are eroded, many grain sizes are removed from the bed simultaneously and in proportions equal to their proportions in the seabed.

T56 Apr
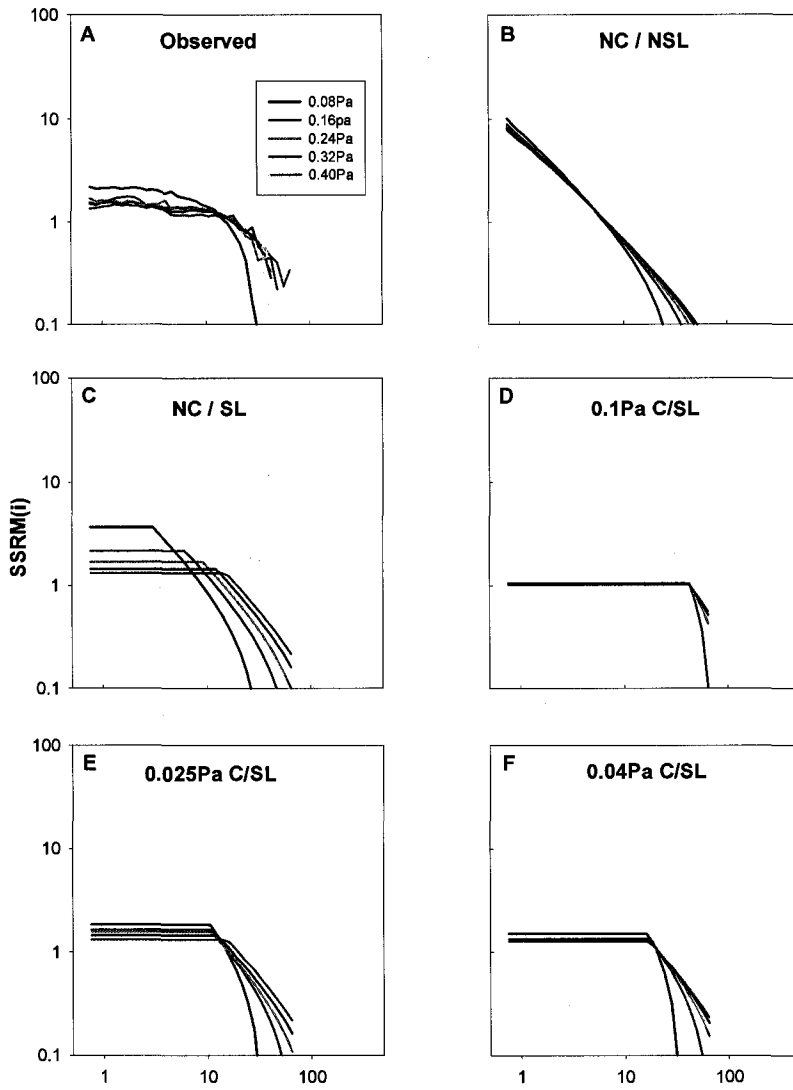
Fig 4.2. Observed and theoretical sediment mobilities for Station T56 in February. Refer to the caption of Figure 4.1 for details.

The model of McCave et al. (1995) is better than that of Wiberg et al. (1994) because it predicts decreasing mobilities for particles greater than 10 μm. Because Wiberg et al. (1994) use 40 μm to discriminate cohesive versus non-cohesive behavior, mobilities decrease only for particles >40 μm, which does not agree with observations (Fig. 4.2 a, d, and e). As well, the Wiberg et al. (1994) model predicts that there is no resuspension during the 0.08Pa shear stress step, while the McCave et. al. (1995) model does.

In summary, at station T56, the cohesive behavior of sediments has to be accounted for in resuspension models to reproduce observed mobilities. Cohesion is also required to explain mobilities for stations seaward of the grain-size transition. The model of McCave et al. (1995) works better than the Wiberg et al. (1994) model because it predicts decreasing mobilities for particles greater than 10 μm.

The erosion of consolidated sediments, as opposed to flocculated "fluff" layers (Thomsen and Gust, 2000), recently has been shown to occur at shear stress values as low as 0.04Pa (Schaff et al., 2006). This value of τ_c corresponds to a grain diameter of 16μm based on the model of Wiberg and Smith, (1987). A value of 0.04Pa is also consistent with some measurements of τ_c for 10 μm grains (White, 1970). Using 0.04Pa as the value of τ_c for all grain sizes smaller than 16 μm (or 10 μm according to White, 1970) yields predicted mobilities similar to those determined using 0.025Pa as the value of τ_c for all grain sizes smaller than 10 μm. Mobilities using the value of $\tau_c = 0.04$ Pa yield slightly better predictions for mobility for the outer shelf stations, which are composed predominantly of mud.

This modeling exercise suggests that limits to sediment availability must be imposed in order to explain observed mobilities. Furthermore, it suggests that cohesion

31

is responsible for the differences in observed mobilities on the Tet Transect. It is important to recognize, however, that the model is highly simplified. Future work in modeling mobility should incorporate other effects such as a stress dependent active layer thickness and the time-dependent consolidation of the bed (e.g., Wiberg et al., 1994; Sanford and Maa, 2001).

4.3 Cohesive Sediments

Cores from the Tet transect show different behaviors with respect to size dependent erosion. One set is modeled well as non-cohesive sediments, and another follows a model for cohesive sediment resuspension. Several definitions exist for distinguishing cohesive from non-cohesive sediments. The simplest is that all sediments that have mean grain sizes less than 63μm are considered cohesive (e.g., Migniot, 1981). Such a definition clearly does not discriminate cohesive versus non-cohesive behavior on the Tet shelf, where all of the sediments had median sizes well below 63μm (Table 3.1). Other definitions focus on the clay content. Mitchell (1976), Dyer (1986) and Raudkivi (1990) suggest that sediments behave cohesively when the % clay found in the sediment rises above 5%-10%. More recently, van Ledden et al. (2004) used a threshold of 7.5% clay (ie. < 4μm) to distinguish cohesive and non-cohesive mixtures. They also used a sand-silt-clay ternary diagram to identify six categories of sediment based on whether the sediment matrix was supported by sand, silt, or clay and whether the sediment was cohesive or non-cohesive. Using this classification system all sediments eroded from the Tet transect fall into category V (i.e., non-cohesive, silt-dominated matrix) or VI (i.e., cohesive, silt-dominated matrix), which were divided by the 7.5% clay (ie. <4μm)

boundary. The sediments eroded from the Tet transect fit the van Ledden classification scheme well. Category V non-cohesive silt mobilities followed the non-cohesive model, and Category VI cohesive silt mobilities matched the cohesive model. (Table 3.1, Figs. 4.1 and 4.2).

4.4 The Sand-Mud Transition

In 1972, McCave proposed that the sand-mud transition (SMT) would form at the boundary where deposition rate of mud exceeds erosion rate by waves and currents. Recently, George et al. (2007) expanded on McCave's arguments by suggesting that at the SMT, deposition rate of mud increases because fragile flocs are no longer destroyed in the highly sheared nearbed flow. This depositional control of the SMT, however, fails to address how the mud and sand remain separated during repeated reworking by waves and currents. Results from this study show that sediment, with a small percentage of clay, can sort under increasing bottom shear stress, with increasingly coarser grains being suspended at increasing stresses. In sediments that contain > 7.5% clay, a wide range of sizes are eroded at equal rates. Sediments with a small clay fraction can be winnowed during erosion, but sediments with a larger clay fraction cannot. With this mechanism an integrated conceptual model of the formation and maintenance of the sand-mud transition emerges.

To produce a deposit with high clay content, a suspension must be flocculated during deposition. Otherwise, the small settling velocities of clay-sized grains makes their settling flux vanishingly small relative to larger grain sizes. As a result, deposits with a high clay content form where nearbed shear is low enough to allow flocs to

survive intact as they settle to the seabed. The abruptness of the SMT arises initially because the extent of flocculation diminishes rapidly with increasing boundary shear stress (Hill et al., 2001). After a single erosion-deposition event, sediment seaward of the SMT has a high clay content because it deposited as flocs. Sediment landward of the SMT has a low clay content because it deposited as single grains. With the arrival of the next transport event, the sediment with low clay content is winnowed of its fine fraction, and the sediment with a high clay content is transported en masse. This differential sorting of the sediment landward and seaward of the SMT accentuates the abruptness of the boundary.

Future work in different locations will clarify the effect of grain size on sortability. The Tet River transect was one where the sediment delivery is low and occurs mostly during flood events. During the time of the study however, there was never a large influx of inorganic material. Sortability studies in an area with large sediment delivery and distinct SMT will help clarify a definition for cohesive versus non-cohesive sediment behavior. As mud is deposited it may change the mobility of bottom sediment and overwhelm the possibility of winnowing its fine grain fraction. Also, if fine grains can be winnowed from sandy environments and all grain sizes are removed from muddy beds at low shear stress, implications for contaminant transport exist. Trace metals and other surface reactive contaminants such as PAH's and PCB's have been shown to have a high affinity for the large surface area of smaller grain sizes. If sediments are exposed to conditions favorable for resuspension and contain harmful contaminants then transport of these materials may occur even at low shear stress.

Chapter 5

Conclusion

Non-cohesive, sandy-silts are prone to sorting because at low shear stresses the clay and fine silt can be winnowed from the sand and coarse silt. Observed mobilities can be approximated by the model of Wiberg et al. (1994) for the stations with low clay content landward of the grain size transition. In contrast, when the fraction of clay in a bottom sediment rises above approximately 7.5 %, the mobility of that sediment approaches 1 across all grain size classes. When eroded, cohesive sediments transport a wide range of grain sizes in suspension in equal concentration proportion to the seabed, even at low shear stress. Effectively, as shear stress increases, so does the mass of sediment eroded, yet the size distribution of sediment in the seabed remains relatively unchanged.

Studies on cohesive sediment transport have shown evidence for the erosion of consolidated bottom sediments at 0.04 Pa, which is equal to the stress required to erode a 16μm sediment grain based on the work of Wiberg and Smith (1987). Modeled mobilities using 16μm as the minimum size for sortable silt are closest to observations. More work will indicate whether this diameter cutoff for "sortability" should be used in place of the 10μm cutoff proposed by McCave et al. (1995) in cohesive transport models.

The difference in the ability to sort cohesive and non-cohesive sediment during erosion may prove to be an important control on the position and maintenance of the sand-mud transition. Non-cohesive muddy sands can have their fine fraction removed at low shear stresses, whereas cohesive sandy muds undergo little sorting, thus maintaining their muddy character.

The change in sediment size and sorting makes the sand-mud transition important acoustically, lithologically, and ecologically. From this study we now have a better understanding of a process that may control the position and maintenance of this unique boundary found on continental shelves and other areas around the world. The ability of sediment to sort or move en masse under different shear stress conditions when composed of specific clay content also has implications for sediment and contaminant transport. Parameters determining cohesive versus non-cohesive behavior based on the percentage of mass with diameters $< 4\mu m$ can easily be inserted into models as a way to distinguish how sediment transport is affected by cohesion.

Future studies will help clarify the effect of grain size on the sortablity of bottom sediment. The modeling in this study was successful in interpreting size-specific relative mobility, but it used a simplified approach that ignores some time dependent variables. With further investigation, data from other areas, and collaboration with sediment modelers, the time dependent variables could be incorporated into models of erosion rates to give a better understanding of sediment transport processes in mixed grain size beds.

References

Amos, C.L., Daborn, G.R., Christian, H.A., Atkinson, A., Robertson, A., 1992. In-situ erosion measurements on fine grained sediments from the Bay of Fundy. Marine Geology. 108, 175-196.

Amos, C.L., Feeney, F., Sutherland, T.F., Luternauer, J.L., 1997. The stability of fine-grained sediments from the Fraser River Delta. Estuarine, Coastal, and Shelf Science. 45, 507-524.

Black, K.S., Tolhurst, T.J., Paterson, D.M., Hagerthy, S.E., 2002. Working with natural cohesive sediments. Journal of Hydraulic Engineering 128, 2-8.

Boss, E., M. S. Twardowski, and S. Herring. 2001. The shape of the particulate beam attenuation spectrum and its relation to the size distribution of oceanic particles. Applied Optics 40, 4885-4893

Curran, K.J., Hill., P.S., Milligan, T.G., 2002. Fine-grained suspended sediment Dynamics in the Eel river flood plume. Continental Shelf Research 22, 2537-2550

Dyer, K.R., 1986. Coastal and Estuarine Sediment Dynamics. Wiley and Sons, Chichester, UK.

Einstein, H.A., 1950. The bed-load function for sediment transportation in open channel flows. United States department of Agriculture, Technical Bulletin, No. 1026.

Fox, J.M., Hill, P.S., Milligan, T.G., Boldrin, A., 2004. Flocculation and sedimentation on the Po River Delta. Marine Geology, 203, 95-107

George, D.A., Hill, P.S., Milligan, T.G., 2007. Flocculation, heavy metals (Cu, Pb, Zn) and the sand-mud transition on the Apennine Margin, Italy. Continental Shelf Research 27, 475-488.

Gust, G., Muller, V., 1997. Interfacial hydrodynamics and entrainment functions of currently used erosion devices. In Burt, N. Parker, R. Watts, J. (Eds.), Cohesive Sediments. Wiley, Chichester, UK, pp. 149-174.

Hill, P. S., Voulgaris, G., Trowbridge, J.H. 2001. Controls on floc size in a continental shelf bottom boundary layer. Journal of Geophysical Research 106, 9543-9549.

Hjulstrom, F., 1939. Transportation of detritus by moving water. In Trask, P.D., (Ed.) Recent Marine Sediments, pp. 5-31.

Kranck, K., Milligan, T.G., 1979. The use of Coulter Counters in Studies of Particle Size Distributions in aquatic Environments. Report Series/ BI-R-79-7/November, 1979: ii+48p.

Kranck, K., 1980. Experiments on the significance of flocculation in the settling of fine-grained sediment in still water. Canadian Journal of Earth Sciences 17, 1517-1526.

Kranck, K., Milligan, T.G., 1991. Grain size in oceanography. In: Syvitski, J.P.M. (Ed.), Principles, Methods, and Application of Particle Size Analysis. Cambridge University Press, New York, pp. 332-345.

Kranck, K., Smith, P.C., Milligan, T.G., 1996b. Grain size characteristics of fine grained unflocculated sediments II: "Multi-round" distributions. Sedimentology. 43, 597-606.

Lynn, V.D., Butman, B., Grant, W.D., 1990. Sediment movement along the US east coast continental shelf-II. Modeling suspended sediment concentrations and transport rates during storms. Continental Shelf Research 10, 429-460

Maa, J.P.Y., Sanford, L.P., Halka, J.P., 1998. Sediment resuspension characteristics in Baltimore Harbour, Maryland. Marine Geology 146, 137-145.

McCave, I.N., 1972. Transport and escape of fine-grained sediment from shelf areas. In Swift. D.J.P. Duane. D.B., Pilkey, O.H. (Eds). Shelf Sediment Transport: Process And Pattern. Dowden, Hutchinson and Ross, 225-247

McCave, I.N., 1984. Size spectra and aggregation of suspended particles in the deep ocean. Deep Sea Research 31, 329-352.

McCave, I.N., Manighetti, B., Robinson, S.G., 1995. Sortable silt and fine sediment size/ composition slicing: parameters for palaeocurrent speed and palaeoceanography. Paleoceanography 10 (3), 593-610.

McCave, I.N., and I.R. Hall, 2006. Size sorting in marine muds: Processes, pitfalls, and Propects for paleaoflow-speed proxies. Geochem. Geophys. Geosyst., 7, Q10N05, doi: 10. 1029/2006GC001284, 37 pp.

Mignoit, C., 1981. Estuarine sediment dynamics- cohesive and non-cohesive materials. Orpington, U.K., Defence Res., Inf. Center. Vol 6, Issue 4, pp. 359-432.

Milligan, T.G., Kranck, K., 1991. Electroresistance particle size analyzers. In: Syvitski, J.P.M. (Ed.), Principles, Methods, and Application of Particle Size Analysis. Cambridge University Press, New York, pp. 109-118.

Milligan, T.G. and D.H. Loring, 1997. The effect of flocculation on the size distributions of bottom sediment in coastal inlets: implications for contaminant transport. Water Air Soil Pollution 99, 33-42.

Milligan, T.G., Hill, P.S., Law, B.A., 2007. Flocculation and the loss of sediment from river plumes. Continental Shelf Research, 27, 309-321.

Mitchell, J.K., 1976. Fundamentals of Soil Behaviour. University of California. Wiley, Berkeley.

Parthenadies, E., 1962. A study of erosion and deposition of cohesive soils in salt water. University of California, Berkely, Ph.D., Thesis, pp. 182.

Postma, H., 1967. Sediment transport and sedimentation in the estuarine environment. In: Lauff, G.H., (Ed), Estuaries, pp. 158-179.

Raudkivi, A.J., 1990. Loose Boundary Hydraulics 3rd Edition. Pergamon Press, Oxford.

Roberts, J.D., Richard, J.A., James, S.C., 2003. Measurements of sediment erosion and transport with the adjustable shear stress erosion and transport flume. Journal of Hydraulic Engineering 129, 862-871.

Sanford, L.P., Maa, J.P.Y., 2001. A unified formulation for fine sediments. Marine Geology 179, 9-23.

Schaaff, E., Grenz, C., Pinazo, C., Lansard, B., 2006. Field and laboratory measurements of sediment erodibility: A comparison. Journal of Sea Research 55, 30-42.

Sheldon, R. W., A. Prakash, and W. H. Sutcliffe, Jr. 1972. The size distribution of particles in the ocean. Limnology and Oceanography 17, 327-339.

Sheldon, R.W., 1972. Size separation of marine seston by membrane and glass fiber filters. Limnology and Oceanography, 17, 494-498.

Shields, A., 1936. Application of the theory of similarity and turbulence research to bedload movement. Mitt. Preuss. Verssuchsanst Wasserbau Schiffbau 26, 5-24.

Smith, J.D. and McLean, S.R., 1977. Spatially averaged flow over a wavy surface. Journal of Geophysical Research 82, 1735-1746.

Soulsby, R., 1997. Dynamics of Marine sands. A Manual for Practical Applications. Thomas Telford Publishing, London.

Sternberg, R.W., Berhane, I., Ogston, A.S., 1999. Measurement of size and settling velocity of suspended aggregates on the Northern California continental shelf. Marine Geology 154, 43-54.

Stevens, A.W., Wheatcroft, R.A., Wiberg, P.L., 2007. Sediment erodibility along the western Adriatic margin, Italy. Continental Shelf Research 27, 400-416

Thomsen, L., Gust, G., 2000. Sediment erosion thresholds and characteristics of resuspended aggregates on the western European continental margin. Deep-Sea Research, Part I 47, 1881-1897.

Tolhurst, T.J., Black, K.S., Shayler, S.A., Mather, S., Black, I., Baker, K., Paterson, D.M., 1999. Measuring the in-situ erosion shear stress of intertidal sediments with the cohesive strength meter (CSM). Estuarine and Coastal Shelf Science, 49, 281-294.

Tolhurst, T.J., Black, K.S., Paterson, D.M., Mitchener, H.J., Termatt, G.R., Shayler, S.A., 2000. A comparison and measurement standardization of four in situ devices for measuring the erosion shear stress of intertidal sediments. Continental Shelf Research 20 (10-11), 1397-1418.

van Ledden, M., W.G.M., van Kesteren, J.C., Winterwerp, 2004. A conceptual framework for the erosion behaviour of sand-mud mixtures. Continental Shelf Research 24, 1-11.

Wheatcroft, R.A., 2002. In situ measurements of near-surface porosity in shallow-water marine sediments. IEEE Journal of Oceanic Engineering 27, 561-570.

White, S.J., 1970. Plane bed thresholds of fine grained sediments. Nature, 228, 152-153.

Wiberg, P.L., Smith, D.J., 1987. Calculations of the critical shear stress for motion of uniform and heterogeneous sediments. Water Resources Research 23, 1471-1478.

Wiberg, P.L., Drake, D.E., Cacchione, D.A., 1994. Sediment resuspension and bed Armoring during high bottom stress events on the northern California inner Continental shelf: measurements and predictions. Continental Shelf Research 14 (10-11), 1191-1219.

Winterwerp, J.C., 1989. Flow induced erosion of cohesive beds. A literature survey. In cohesive sediments (Rep. 25). Delft. Wl/Delft Hydraulics and Rijwaterstaat.

Zwolsman, J.J.G., van Eck, G.T.M., Burger, G., 1996. Spatial and temporal distribution of trace metals in sediments from the Scheldt Estuary, South-west Netherlands. Estuarine and Coastal Shelf Science 43, 55-79.

Appendix A

Table of all Station Locations

List of all station locations for slo-core core samples collected along the Tet transect for all three sampling periods that were either eroded using the Gust microcosm erosion chamber or used to analyze grain-size from the top 0.5cm of uneroded bottom sediment.

Date	Stn #	Water Depth (m)	Latitude (N)	Longitude (E)	Core Function
Oct-04	T20A	20	42.7032	3.0553	Eroded Gust Chamber
Oct-04	T20C	20	42.7038	3.0547	Core Surficial Grain Size
Oct-04	T20E	20	42.7044	3.0548	Core Surficial Grain Size
Oct-04	T28E	28	42.6999	3.0657	Eroded Gust Chamber
Oct-04	T28C	28	42.7033	3.0728	Core Surficial Grain Size
Oct-04	T28D	28	42.7000	3.0656	Core Surficial Grain Size
Oct-04	T35B	35	42.6983	3.0942	Eroded Gust Chamber
Oct-04	T35C	35	42.6983	3.0944	Core Surficial Grain Size
Oct-04	T35E	35	42.6980	3.0943	Core Surficial Grain Size
Oct-04	T40A	40	42.6938	3.1087	Core Surficial Grain Size
Oct-04	T40B	40	42.6938	3.1094	Core Surficial Grain Size
Oct-04	T45C	45	42.6879	3.1244	Eroded Gust Chamber
Oct-04	T45B	45	42.6883	3.1243	Core Surficial Grain Size
Oct-04	T45F	45	42.6888	3.1245	Core Surficial Grain Size
Oct-04	T56D	56	42.6768	3.1667	Eroded Gust Chamber
Oct-04	T56B	56	42.6760	3.1666	Core Surficial Grain Size
Oct-04	T56C	56	42.6762	3.1668	Core Surficial Grain Size
Feb-05	T20C	19	42.7047	3.0526	Eroded Gust Chamber
Feb-05	T20G	21	42.7047	3.0538	Eroded Gust Chamber
Feb-05	T20E	20	42.7045	3.0547	Core Surficial Grain Size
Feb-05	T20F	19	42.7048	3.0541	Core Surficial Grain Size
Feb-05	T28C	28	42.7050	3.1012	Eroded Gust Chamber
Feb-05	T28F	28	42.7044	3.0695	Eroded Gust Chamber
Feb-05	T28M	27	42.7021	3.0651	Eroded Gust Chamber
Feb-05	T28B	28	42.7050	3.1012	Core Surficial Grain Size
Feb-05	T28D	28	42.7053	3.0690	Core Surficial Grain Size
Feb-05	T28L	27	42.6989	3.0661	Core Surficial Grain Size
Feb-05	T35A	35	42.6974	3.1292	Eroded Gust Chamber
Feb-05	T35E	35	42.6979	3.0934	Eroded Gust Chamber
Feb-05	T35I	35	42.6983	3.0961	Eroded Gust Chamber
Feb-05	T35B	35	42.6985	3.0945	Core Surficial Grain Size
Feb-05	T35C	35	42.6987	3.0946	Core Surficial Grain Size
Feb-05	T35H	35	42.6969	3.0999	Core Surficial Grain Size
Feb-05	T40B	40	42.7103	3.1079	Eroded Gust Chamber
Feb-05	T40G	40	42.6953	3.1118	Eroded Gust Chamber
Feb-05	T40D	40	42.6935	3.1073	Core Surficial Grain Size
Feb-05	T40E	40	42.6938	3.1085	Core Surficial Grain Size
Feb-05	T45B	46	42.6894	3.1240	Eroded Gust Chamber
Feb-05	T45D	47	42.6867	3.1245	Eroded Gust Chamber
Feb-05	T45H	46	42.6867	3.1246	Eroded Gust Chamber
Feb-05	T45A	46	42.6888	3.1229	Core Surficial Grain Size
Feb-05	T45E	47	42.6880	3.1243	Core Surficial Grain Size
Feb-05	T45I	46	42.6870	3.1251	Core Surficial Grain Size
Feb-05	T56A	56	42.6753	3.1689	Eroded Gust Chamber
Feb-05	T56E	56	42.6752	3.1685	Eroded Gust Chamber
Feb-05	T56I	56	42.6775	3.1680	Eroded Gust Chamber
Feb-05	T56C	56	42.6761	3.1678	Core Surficial Grain Size
Feb-05	T56F	56	42.6757	3.1673	Core Surficial Grain Size
Feb-05	T56K	56	42.6763	3.1676	Core Surficial Grain Size
Feb-05	T74B	74	42.6642	3.2099	Eroded Gust Chamber
Feb-05	T74H	73	42.6643	3.2066	Eroded Gust Chamber

Feb-05	T74D	74	42.6639	3.2099	Eroded Gust Chamber
Feb-05	T74C	74	42.6631	3.2110	Core Surficial Grain Size
Feb-05	T74G	74	42.6648	3.2087	Core Surficial Grain Size
Feb-05	T74E	74	42.6644	3.2097	Core Surficial Grain Size
Apr-05	T20B	22	42.7053	3.0560	Eroded Gust Chamber
Apr-05	T20H	21	42.7031	3.0549	Eroded Gust Chamber
Apr-05	T20I	21	42.7032	3.0548	Eroded Gust Chamber
Apr-05	T20C	22	42.7024	3.0562	Core Surficial Grain Size
Apr-05	T20D	23	42.7038	3.0575	Core Surficial Grain Size
Apr-05	T20F	21	42.7020	3.0544	Core Surficial Grain Size
Apr-05	T28B	28	42.7043	3.0724	Eroded Gust Chamber
Apr-05	T28J	28	42.7037	3.0726	Eroded Gust Chamber
Apr-05	T28G	28	42.7033	3.0732	Eroded Gust Chamber
Apr-05	T28E	28	42.7047	3.0713	Core Surficial Grain Size
Apr-05	T28K	28	42.7035	3.0732	Core Surficial Grain Size
Apr-05	T28C	28	42.7039	3.0723	Core Surficial Grain Size
Apr-05	T35B	35	42.6976	3.0949	Eroded Gust Chamber
Apr-05	T35H	36	42.6990	3.0956	Eroded Gust Chamber
Apr-05	T35I	35	42.6984	3.0944	Eroded Gust Chamber
Apr-05	T35C	35	42.6988	3.0948	Core Surficial Grain Size
Apr-05	T35J	35	42.6978	3.0948	Core Surficial Grain Size
Apr-05	T35A	36	42.7000	3.0964	Core Surficial Grain Size
Apr-05	T40C	40	42.6945	3.1086	Eroded Gust Chamber
Apr-05	T40H	40	42.6950	3.1083	Eroded Gust Chamber
Apr-05	T40I	40	42.6933	3.1100	Eroded Gust Chamber
Apr-05	T40D	40	42.6926	3.1079	Core Surficial Grain Size
Apr-05	T40J	40	42.6950	3.1100	Core Surficial Grain Size
Apr-05	T40F	40	42.6946	3.1101	Core Surficial Grain Size
Apr-05	T45B	46	42.6889	3.1247	Eroded Gust Chamber
Apr-05	T45I	47	42.6894	3.1249	Eroded Gust Chamber
Apr-05	T45D	46	42.6885	3.1237	Eroded Gust Chamber
Apr-05	T45C	46	42.6898	3.1237	Core Surficial Grain Size
Apr-05	T45H	45	42.6888	3.1250	Core Surficial Grain Size
Apr-05	T45E	46	42.6893	3.1248	Core Surficial Grain Size
Apr-05	T56B	58	42.6756	3.1700	Eroded Gust Chamber
Apr-05	T56X	56	42.6758	3.1686	Eroded Gust Chamber
Apr-05	T56E	58	42.6776	3.1705	Eroded Gust Chamber
Apr-05	T56A	58	42.6780	3.1707	Core Surficial Grain Size
Apr-05	T56Y	56	42.6755	3.1689	Core Surficial Grain Size
Apr-05	T56F	57	42.6777	3.1683	Core Surficial Grain Size
Apr-05	T74A	75	42.6641	3.2108	Eroded Gust Chamber
Apr-05	T74K	72	42.6633	3.2111	Eroded Gust Chamber
Apr-05	T74F	75	42.6681	3.2126	Eroded Gust Chamber
Apr-05	T74D	75	42.6653	3.2087	Core Surficial Grain Size
Apr-05	T74H	75	42.6632	3.2100	Core Surficial Grain Size
Apr-05	T74G	76	42.6687	3.2129	Core Surficial Grain Size

Appendix B

Grain-Size Analysis

Data listed in appendix B are the results of grain size analysis carried out in the Particle Dynamics Lab at the Bedford Institute of Oceanography using a Coulter Multisizer IIe electroresistant particle size analyzer. Data are for stations occupied along the Tet transect and list the volume fractions in suspension for each applied shear stress. At the end of each Table is the average grain size data of the bottom sediment for the specific station along the Transect. Bottom sediment averages are used to smooth spatial changes in sediment texture over very short distances. The stations that were occupied and run for bottom sediment analysis are listed in Appendix A. The average bottom sediment value for a specific station is listed because it is needed to calculate size-specific relative mobility. Using the data listed in the tables of appendix B, size-specific relative mobility can be calculated for each station by dividing the size-specific volume fraction for each erosion step at a specific station location by the size-specific volume fraction in the bottom sediment for that station.

Station ID	T20A	T20A	T20A	T20A	T20A	T20 Avg
Stress	0.08	0.16	0.24	0.32	0.4	Bot Sed
Date	Oct-04	Oct-04	Oct-04	Oct-04	Oct-04	Oct-04
Diameter (um)						
0.76	5.08	1.69	0.55	0.58	0.46	0.40
0.87	4.61	1.70	0.59	0.63	0.52	0.47
1.00	4.78	1.81	0.66	0.70	0.57	0.48
1.15	4.91	1.91	0.73	0.75	0.63	0.48
1.32	4.19	1.96	0.79	0.82	0.68	0.51
1.52	4.14	2.13	0.87	0.88	0.75	0.54
1.74	4.29	2.20	0.94	0.96	0.81	0.61
2.00	3.76	2.34	1.02	1.05	0.90	0.66
2.30	4.01	2.35	1.08	1.11	0.95	0.76
2.64	4.57	2.75	1.19	1.20	1.04	0.81
3.03	5.51	2.68	1.33	1.31	1.16	0.97
3.48	7.01	2.99	1.50	1.41	1.14	1.11
4.00	5.06	2.87	1.64	1.61	1.36	1.28
4.59	6.66	3.07	1.88	1.74	1.55	1.34
5.28	6.14	3.41	2.18	1.97	1.79	1.40
6.06	5.42	3.67	2.47	2.27	2.10	1.66
6.96	3.02	3.89	2.88	2.63	2.41	2.00
8.00	2.15	4.27	3.29	3.02	2.78	2.30
9.19	2.32	4.47	3.71	3.40	3.30	2.62
10.56	2.11	4.54	4.07	3.73	3.45	3.08
12.13	2.57	4.96	4.79	4.24	3.93	3.52
13.93	1.77	5.00	5.28	4.72	4.35	3.87
16.00	1.99	5.40	5.96	5.31	4.95	4.30
18.38	2.06	5.65	6.41	5.78	5.54	4.52
21.11	0.39	5.14	7.08	6.25	5.95	4.95
24.25	1.49	4.65	6.95	6.36	6.47	5.32
27.86		4.62	6.48	6.46	6.43	5.48
32.00		3.95	5.98	6.35	5.62	5.73
36.76		2.46	4.99	5.59	6.16	6.01
42.22		1.21	4.06	4.95	4.59	5.24
48.50		0.23	3.11	3.98	4.81	5.01
55.72			1.90	3.76	3.92	4.93
64.00			2.06	2.80	3.82	5.16
73.52			1.56	1.72	3.41	2.90
84.45					1.68	3.33
97.01						2.72
111.43						3.54
128.00						

Station ID	T28E	T28E	T28E	T28E		T28 Avg
Stress	0.08	0.16	0.24	0.32		Bot Sed
Date	Oct-04	Oct-04	Oct-04	Oct-04	Oct-04	Oct-04
Diameter (um)						
0.76	3.33	1.09	0.55	0.46		
0.87	3.62	1.23	0.59	0.50		0.28
1.00	4.04	1.38	0.65	0.56		0.31
1.15	4.21	1.44	0.71	0.60		0.33
1.32	4.50	1.60	0.76	0.63		0.34
1.52	4.70	1.69	0.83	0.69		0.37
1.74	4.99	1.83	0.91	0.74		0.38
2.00	5.09	2.08	0.97	0.83		0.40
2.30	5.19	2.33	1.04	0.90		0.42
2.64	4.95	2.33	1.12	0.99		0.45
3.03	5.06	2.64	1.23	1.11		0.51
3.48	4.49	2.93	1.34	1.25		0.54
4.00	3.98	3.27	1.57	1.29		0.58
4.59	3.83	3.82	1.81	1.48		0.66
5.28	4.05	4.19	2.08	1.74		0.72
6.06	4.04	4.77	2.34	2.00		0.83
6.96	3.92	5.17	2.56	2.31		0.97
8.00	3.94	5.62	2.80	2.51		1.14
9.19	3.65	5.91	3.00	2.69		1.31
10.56	3.61	5.86	3.15	2.99		1.50
12.13	3.67	5.97	3.44	3.19		1.68
13.93	2.91	5.49	3.91	3.22		1.88
16.00	2.66	5.90	3.83	3.40		2.20
18.38	1.79	5.15	4.03	3.79		2.33
21.11	1.48	3.25	4.22	3.87		2.72
24.25	1.27	3.50	4.22	4.11		3.03
27.86	0.78	2.98	4.35	4.38		3.78
32.00	0.25	2.26	4.36	4.78		4.70
36.76		2.46	5.18	5.82		5.73
42.22		1.58	6.03	6.03		7.35
48.50		0.25	6.53	7.82		9.97
55.72			8.08	9.24		12.52
64.00			6.69	7.32		12.99
73.52			3.19	4.84		9.78
84.45			1.92	1.90		5.44
97.01						1.85
111.43						
128.00						

Station ID	T35B	T35B	T35B	T35B	T35B	T35 Avg
Stress	0.08	0.16	0.24	0.32	0.40	Bot Sed
Date	Oct-04	Oct-04	Oct-04	Oct-04	Oct-04	Oct-04
Diameter (um)						
0.76	3.70	0.70	0.48	0.34	0.41	0.30
0.87	3.92	0.75	0.53	0.36	0.46	0.32
1.00	4.23	0.81	0.57	0.39	0.48	0.34
1.15	4.58	0.86	0.60	0.41	0.52	0.35
1.32	4.74	0.86	0.64	0.44	0.56	0.38
1.52	4.92	0.94	0.70	0.46	0.61	0.40
1.74	5.14	1.01	0.76	0.51	0.66	0.41
2.00	5.39	1.03	0.79	0.54	0.71	0.45
2.30	5.19	1.16	0.87	0.58	0.77	0.51
2.64	5.52	1.18	0.93	0.62	0.82	0.53
3.03	5.24	1.30	0.95	0.68	0.92	0.56
3.48	5.07	1.39	0.99	0.71	0.88	0.61
4.00	4.58	1.57	1.15	0.78	0.95	0.73
4.59	4.55	1.69	1.13	0.90	1.07	0.80
5.28	4.66	1.87	1.35	1.05	1.26	0.83
6.06	4.56	2.20	1.62	1.22	1.47	0.95
6.96	4.08	2.41	1.88	1.38	1.72	1.08
8.00	3.57	2.68	2.13	1.57	1.89	1.21
9.19	3.08	2.89	2.38	1.70	2.11	1.34
10.56	2.50	3.21	2.70	1.88	2.40	1.49
12.13	2.56	3.26	2.97	1.99	2.62	1.70
13.93	2.27	3.51	3.29	2.27	3.05	1.91
16.00	1.58	3.64	3.47	2.62	3.33	2.06
18.38	1.21	3.78	3.71	2.94	3.82	2.41
21.11	1.11	4.18	4.10	3.31	4.45	2.82
24.25	1.04	4.40	4.50	3.76	5.04	3.18
27.86	0.99	4.71	4.89	4.44	5.63	4.01
32.00		5.09	5.94	5.79	6.82	5.14
36.76		5.87	7.16	7.62	8.38	7.23
42.22		6.45	8.75	9.68	9.02	10.16
48.50		6.93	9.66	12.06	9.38	12.61
55.72		6.45	8.52	11.97	7.23	12.87
64.00		5.38	5.18	8.43	5.88	10.46
73.52		3.91	3.27	4.54	2.85	5.62
84.45		1.94	1.47	2.06	1.82	3.26
97.01						0.95
111.43						
128.00						

Station ID	T45C	T45C	T45C	T45C	T45C	T45 Avg
Stress	0.08	0.16	0.24	0.32	0.40	Bot Sed
Date	Oct-04	Oct-04	Oct-04	Oct-04	Oct-04	Oct-04
Diameter (um)						
0.76	2.67	1.26	1.06	1.03	0.77	0.81
0.87	2.80	1.35	1.10	1.08	0.82	0.87
1.00	2.84	1.42	1.21	1.14	0.88	0.96
1.15	2.86	1.47	1.27	1.21	0.96	1.01
1.32	2.87	1.55	1.31	1.25	0.98	1.07
1.52	2.81	1.64	1.37	1.35	1.05	1.15
1.74	2.93	1.75	1.40	1.44	1.12	1.21
2.00	2.92	1.82	1.52	1.49	1.21	1.26
2.30	2.85	1.84	1.59	1.56	1.24	1.43
2.64	3.01	2.16	1.75	1.74	1.33	1.50
3.03	3.11	2.34	1.77	1.76	1.39	1.51
3.48	3.30	2.72	2.06	2.03	1.52	1.76
4.00	2.98	2.78	2.20	2.29	1.73	1.98
4.59	3.63	3.45	2.70	2.62	1.92	2.08
5.28	3.77	3.94	3.13	3.07	2.18	2.19
6.06	3.66	4.55	3.64	3.48	2.54	2.57
6.96	3.51	5.01	4.17	3.93	2.85	2.93
8.00	3.31	5.33	4.44	4.28	3.16	3.21
9.19	3.19	5.52	4.65	4.49	3.36	3.50
10.56	3.39	5.64	4.79	4.48	3.66	3.72
12.13	3.64	5.24	4.83	4.63	3.82	4.02
13.93	4.23	4.89	4.88	4.88	4.18	4.39
16.00	3.81	4.43	5.04	4.76	4.33	4.40
18.38	2.97	4.30	5.37	4.86	4.59	4.28
21.11	3.16	3.78	4.90	5.31	4.94	4.96
24.25	3.39	3.28	4.97	4.69	5.26	4.95
27.86	2.39	2.45	4.99	4.76	5.25	5.27
32.00	1.24	2.64	4.67	5.65	6.14	5.60
36.76	0.59	1.83	3.97	4.28	5.69	5.70
42.22	2.24	2.32	3.42	4.00	6.03	5.26
48.50	3.24	2.33	1.83	2.77	5.72	5.32
55.72	2.56	2.78	2.48	2.18	4.56	3.87
64.00	4.13	2.21	1.51	1.52	3.11	2.82
73.52					1.71	1.37
84.45						1.07
97.01						
111.43						
128.00						

Station ID	T56D	T56D	T56D	T56D	T56D	T56 Avg
Stress	0.08	0.16	0.24	0.32	0.40	Bot Sed
Date	Oct-04	Oct-04	Oct-04	Oct-04	Oct-04	Oct-04
Diameter (um)						
0.76	1.76	1.26	1.30	1.02	0.96	1.15
0.87	1.81	1.34	1.37	1.04	0.99	1.15
1.00	1.92	1.44	1.47	1.07	1.07	1.21
1.15	2.09	1.53	1.51	1.12	1.12	1.22
1.32	2.12	1.64	1.58	1.16	1.19	1.27
1.52	2.25	1.69	1.73	1.24	1.31	1.32
1.74	2.50	1.82	1.95	1.40	1.40	1.35
2.00	2.64	1.97	2.17	1.53	1.47	1.45
2.30	2.62	1.99	2.08	1.41	1.62	1.57
2.64	2.61	2.22	2.32	1.59	1.56	1.68
3.03	2.81	2.32	2.20	1.65	1.81	1.71
3.48	3.55	2.60	2.59	1.96	1.96	1.99
4.00	3.72	2.81	2.95	2.01	2.12	2.04
4.59	3.56	3.12	3.11	2.33	2.42	2.15
5.28	4.45	3.66	4.10	2.77	2.96	2.49
6.06	5.10	4.27	3.52	3.25	3.40	2.87
6.96	5.87	4.85	4.05	3.78	3.93	3.32
8.00	6.02	5.46	4.46	4.20	4.57	3.68
9.19	6.31	5.92	4.84	4.73	5.13	4.22
10.56	6.23	6.11	5.12	5.01	5.25	4.43
12.13	5.69	6.24	5.44	5.52	5.69	4.64
13.93	5.44	5.95	5.43	5.88	5.93	4.78
16.00	4.75	5.73	5.41	5.93	6.00	5.09
18.38	3.77	5.28	5.29	5.91	6.11	5.14
21.11	3.10	4.47	5.12	5.72	5.80	5.52
24.25	2.47	3.85	4.31	5.39	5.33	5.53
27.86	1.87	3.55	4.18	4.90	4.97	5.28
32.00	1.35	2.39	3.37	5.09	3.88	4.99
36.76	1.62	1.69	2.73	3.71	3.01	4.63
42.22		1.23	2.62	3.24	2.59	3.86
48.50		0.77	1.69	2.79	2.99	3.29
55.72		0.84		1.65	1.44	2.28
64.00						1.52
73.52						1.19
84.45						1.07
97.01						
111.43						
128.00						

Station ID	T20G	T20G	T20G	T20G	T20G	T20 Avg
Stress	0.08	0.16	0.24	0.32	0.40	Bot Sed
Date	Feb-05	Feb-05	Feb-05	Feb-05	Feb-05	Feb-05
Diameter (um)						
0.76	0.39	0.44	0.61	0.45	0.48	0.21
0.87	0.46	0.49	0.68	0.51	0.54	0.24
1.00	0.52	0.55	0.76	0.57	0.61	0.28
1.15	0.59	0.57	0.81	0.62	0.67	0.32
1.32	0.64	0.66	0.90	0.67	0.75	0.37
1.52	0.70	0.71	0.95	0.71	0.82	0.41
1.74	0.78	0.76	1.05	0.78	0.87	0.49
2.00	0.90	0.85	1.14	0.83	0.93	0.56
2.30	0.97	0.96	1.20	0.91	1.07	0.64
2.64	1.12	1.08	1.33	0.98	1.18	0.74
3.03	1.26	1.20	1.45	1.09	1.27	0.84
3.48	1.36	1.29	1.55	1.23	1.39	0.97
4.00	1.56	1.55	1.66	1.30	1.49	1.06
4.59	1.86	1.72	1.80	1.42	1.69	1.20
5.28	2.20	2.05	2.08	1.45	2.01	1.33
6.06	2.57	2.38	2.39	1.57	2.34	1.61
6.96	2.92	2.69	2.74	1.83	2.59	1.83
8.00	3.59	2.97	3.06	2.05	2.89	2.11
9.19	3.62	3.15	3.21	2.22	3.27	2.37
10.56	3.92	3.19	3.52	2.42	3.61	2.62
12.13	4.21	3.49	3.63	2.48	3.88	2.88
13.93	4.53	3.72	3.84	2.77	4.27	3.08
16.00	4.72	3.77	4.10	3.11	4.59	3.27
18.38	4.41	3.91	4.24	3.44	5.01	3.59
21.11	4.83	3.99	4.64	3.70	5.22	3.88
24.25	4.84	3.80	4.40	3.98	5.65	4.06
27.86	4.10	3.82	4.79	4.31	5.55	4.15
32.00	3.82	4.07	4.85	4.64	5.56	3.90
36.76	3.84	4.46	4.80	5.28	5.91	4.08
42.22	4.88	5.80	4.51	6.20	4.67	4.41
48.50	4.57	5.91	5.22	5.48	5.31	4.74
55.72	5.69	6.33	5.78	7.27	4.90	4.81
64.00	5.43	7.76	5.10	7.70	4.01	5.04
73.52	4.02	4.65	4.50	7.34	3.45	5.64
84.45	4.19	5.26	2.71	5.65	1.56	5.91
97.01				3.04		5.27
111.43						5.26
128.00						4.34

51

Station ID	T20C	T20C	T20C	T20C		T20 Avg
Stress	0.08	0.16	0.24	0.32		Bot Sed
Date	Feb-05	Feb-05	Feb-05	Feb-05		Feb-05
Diameter (um)						
0.76		0.95	0.58	0.45		0.21
0.87	1.49	0.97	0.62	0.48		0.24
1.00	1.37	1.00	0.67	0.52		0.28
1.15	1.43	1.09	0.73	0.58		0.32
1.32	1.42	1.19	0.80	0.66		0.37
1.52	1.43	1.26	0.88	0.73		0.41
1.74	1.42	1.41	0.96	0.79		0.49
2.00	1.65	1.56	1.08	0.89		0.56
2.30	1.72	1.59	1.20	0.96		0.64
2.64	1.81	1.87	1.31	1.06		0.74
3.03	2.01	2.11	1.39	1.22		0.84
3.48	2.16	2.19	1.63	1.30		0.97
4.00	2.09	2.41	1.81	1.52		1.06
4.59	2.65	2.74	1.91	1.62		1.20
5.28	2.94	3.12	2.06	1.89		1.33
6.06	3.29	3.55	2.47	2.21		1.61
6.96	3.68	3.92	2.79	2.53		1.83
8.00	3.83	4.44	3.18	2.94		2.11
9.19	4.13	4.69	3.48	3.21		2.37
10.56	4.15	4.92	3.72	3.62		2.62
12.13	4.25	5.22	4.14	3.92		2.88
13.93	3.70	5.34	3.99	4.16		3.08
16.00	4.35	5.14	4.54	4.53		3.27
18.38	4.53	5.07	4.70	4.61		3.59
21.11	4.47	4.92	5.00	5.37		3.88
24.25	4.37	4.57	4.85	5.51		4.06
27.86	4.69	4.22	5.10	5.81		4.15
32.00	4.49	3.87	5.39	5.65		3.90
36.76	4.62	3.24	5.16	5.36		4.08
42.22	4.86	3.32	5.12	6.10		4.41
48.50	5.64	2.92	5.84	5.58		4.74
55.72	5.37	2.12	5.19	4.71		4.81
64.00		1.40	4.80	4.47		5.04
73.52		1.64	2.91	3.15		5.64
84.45				1.90		5.91
97.01						5.27
111.43						5.26
128.00						4.34

Station ID	T28F	T28F	T28F	T28F	T28F	T28 Avg
Stress	0.08	0.16	0.24	0.32	0.40	Bot Sed
Date	Feb-05	Feb-05	Feb-05	Feb-05	Feb-05	Feb-05
Diameter (um)						
0.76	2.51	1.01	0.63	0.49	0.33	0.22
0.87	2.70	1.15	0.71	0.52	0.34	0.24
1.00	2.83	1.19	0.76	0.56	0.35	0.26
1.15	2.98	1.31	0.82	0.60	0.37	0.28
1.32	3.18	1.39	0.88	0.68	0.40	0.29
1.52	3.39	1.51	0.96	0.73	0.42	0.30
1.74	3.53	1.62	1.03	0.78	0.45	0.31
2.00	3.55	1.76	1.09	0.85	0.50	0.34
2.30	3.86	1.87	1.17	0.95	0.52	0.37
2.64	3.80	2.01	1.31	0.99	0.55	0.41
3.03	4.06	2.26	1.37	1.00	0.59	0.45
3.48	4.26	2.28	1.50	1.12	0.61	0.48
4.00	4.24	2.54	1.79	1.16	0.72	0.57
4.59	3.89	2.66	1.81	1.21	0.86	0.61
5.28	3.94	3.02	2.04	1.36	0.93	0.70
6.06	4.07	3.40	2.32	1.55	1.06	0.82
6.96	4.30	3.81	2.61	1.78	1.26	0.96
8.00	4.25	4.04	2.92	1.99	1.39	1.12
9.19	4.13	4.34	3.20	2.19	1.63	1.28
10.56	4.21	4.55	3.49	2.38	1.78	1.40
12.13	3.71	4.30	3.69	2.70	1.93	1.58
13.93	3.49	4.69	3.90	2.82	2.10	1.85
16.00	3.31	4.34	4.14	3.08	2.42	2.07
18.38	2.84	4.44	4.39	3.45	3.04	2.37
21.11	1.91	4.15	4.85	3.94	3.46	2.57
24.25	2.58	3.87	5.64	4.50	4.25	3.17
27.86	1.86	3.30	5.95	5.57	4.92	3.67
32.00	3.80	3.26	6.59	6.81	6.44	4.30
36.76	2.84	3.78	7.16	8.13	8.18	6.16
42.22		4.29	7.00	10.37	10.46	8.59
48.50		4.26	5.98	10.50	12.81	12.37
55.72		3.69	4.85	8.08	11.61	15.69
64.00		2.36	2.24	5.22	7.43	12.56
73.52		1.54	1.21	1.94	4.19	7.81
84.45					1.69	3.17
97.01						0.64
111.43						
128.00						

Station ID	T28C	T28C	T28C	T28C	T28C	T28 Avg
Stress	0.08	0.16	0.24	0.32	0.40	Bot Sed
Date	Feb-05	Feb-05	Feb-05	Feb-05	Feb-05	Feb-05
Diameter (um)						
0.76	1.71	0.83	0.47	0.45	0.41	0.22
0.87	1.84	0.90	0.52	0.48	0.44	0.24
1.00	1.99	1.00	0.58	0.53	0.48	0.26
1.15	2.17	1.07	0.64	0.57	0.54	0.28
1.32	2.30	1.17	0.70	0.60	0.58	0.29
1.52	2.50	1.25	0.74	0.67	0.63	0.30
1.74	2.63	1.26	0.78	0.66	0.66	0.31
2.00	2.79	1.38	0.83	0.72	0.70	0.34
2.30	3.06	1.45	0.85	0.77	0.75	0.37
2.64	3.34	1.62	0.96	0.81	0.77	0.41
3.03	3.45	1.71	1.00	0.89	0.82	0.45
3.48	3.60	1.75	1.05	1.00	0.84	0.48
4.00	3.84	1.93	1.23	1.01	0.95	0.57
4.59	4.12	2.19	1.46	1.10	1.04	0.61
5.28	4.20	2.54	1.68	1.28	1.15	0.70
6.06	4.54	2.88	1.85	1.42	1.34	0.82
6.96	4.56	3.15	2.10	1.53	1.47	0.96
8.00	4.57	3.41	2.34	1.68	1.56	1.12
9.19	4.36	3.68	2.44	1.81	1.70	1.28
10.56	4.25	3.80	2.67	1.97	1.90	1.40
12.13	4.42	4.04	2.86	2.04	2.00	1.58
13.93	4.06	4.08	3.21	2.54	2.26	1.85
16.00	3.89	4.40	3.55	2.56	2.32	2.07
18.38	3.73	4.72	3.91	2.98	2.59	2.37
21.11	3.33	4.22	4.05	3.17	3.15	2.57
24.25	3.06	4.76	4.32	3.73	3.56	3.17
27.86	2.52	4.63	4.63	3.88	4.02	3.67
32.00	1.85	4.23	5.00	4.35	4.79	4.30
36.76	2.07	5.06	5.52	5.86	6.05	6.16
42.22	2.20	4.43	7.78	7.23	7.32	8.59
48.50	1.96	4.88	8.45	9.08	8.92	12.37
55.72	1.10	4.74	9.61	12.69	10.22	15.69
64.00		3.46	8.68	10.27	10.78	12.56
73.52		3.40	3.51	6.94	6.64	7.81
84.45				2.73	4.71	3.17
97.01					1.97	0.64
111.43						
128.00						

Station ID	T35A	T35A	T35A	T35A	T35A	T35 Avg
Stress	0.08	0.16	0.24	0.32	0.40	Bot Sed
Date	Feb-05	Feb-05	Feb-05	Feb-05	Feb-05	Feb-05
Diameter (um)						
0.76	1.86	1.52	0.62	0.34	0.31	0.41
0.87	1.98	1.56	0.67	0.37	0.34	0.43
1.00	2.06	1.66	0.74	0.41	0.37	0.47
1.15	2.14	1.76	0.82	0.45	0.39	0.51
1.32	2.17	1.81	0.84	0.47	0.42	0.55
1.52	2.17	1.93	0.87	0.52	0.44	0.59
1.74	2.30	2.13	0.97	0.55	0.47	0.62
2.00	2.30	2.24	0.96	0.59	0.50	0.67
2.30	2.54	2.35	1.04	0.61	0.55	0.73
2.64	2.53	2.50	1.16	0.66	0.57	0.82
3.03	2.86	2.81	1.26	0.70	0.62	0.85
3.48	3.02	2.70	1.31	0.80	0.66	0.93
4.00	3.12	3.12	1.37	0.84	0.71	1.01
4.59	3.27	3.13	1.66	0.99	0.75	1.07
5.28	3.54	3.38	1.89	1.16	0.85	1.17
6.06	3.73	3.70	2.26	1.32	0.99	1.35
6.96	3.87	3.98	2.50	1.60	1.08	1.55
8.00	3.78	4.03	2.79	1.76	1.21	1.71
9.19	4.09	4.16	2.90	2.04	1.29	1.86
10.56	4.22	4.14	3.29	2.04	1.46	1.98
12.13	4.33	3.95	3.70	2.45	1.61	2.06
13.93	4.57	4.06	4.12	2.80	1.84	2.21
16.00	4.15	3.86	4.34	2.98	2.13	2.31
18.38	3.91	3.81	4.58	3.39	2.45	2.33
21.11	3.86	4.07	4.63	3.56	2.84	2.59
24.25	3.49	3.81	5.14	4.03	3.28	3.09
27.86	3.31	3.73	5.39	4.58	3.89	3.78
32.00	3.10	3.54	5.34	5.61	4.76	4.73
36.76	3.17	3.32	6.01	6.73	6.57	6.40
42.22	3.91	3.66	7.47	9.16	8.68	9.04
48.50	2.02	3.92	8.99	10.73	12.54	11.47
55.72	2.60	2.32	7.34	11.99	13.94	12.07
64.00		1.32	3.04	8.52	10.82	9.58
73.52				4.06	6.50	5.58
84.45				1.20	4.19	2.65
97.01						0.82
111.43						
128.00						

Station ID	T35E	T35E	T35E	T35E	T35E	T35 Avg
Stress	0.08	0.16	0.24	0.32	0.40	Bot Sed
Date	Feb-05	Feb-05	Feb-05	Feb-05	Feb-05	Feb-05
Diameter (um)						
0.76	0.75	0.87	0.45	0.38	0.42	0.41
0.87	0.79	0.90	0.47	0.40	0.44	0.43
1.00	0.82	0.95	0.51	0.42	0.47	0.47
1.15	0.88	1.05	0.56	0.47	0.51	0.51
1.32	0.94	1.12	0.62	0.50	0.57	0.55
1.52	0.98	1.22	0.67	0.57	0.61	0.59
1.74	1.03	1.25	0.75	0.59	0.67	0.62
2.00	1.06	1.40	0.77	0.64	0.70	0.67
2.30	1.22	1.44	0.90	0.70	0.74	0.73
2.64	1.32	1.48	0.93	0.76	0.81	0.82
3.03	1.35	1.64	1.04	0.83	0.92	0.85
3.48	1.32	1.80	1.20	0.95	0.96	0.93
4.00	1.58	2.13	1.30	1.05	0.95	1.01
4.59	1.74	2.11	1.45	1.13	1.04	1.07
5.28	1.95	2.41	1.69	1.18	1.21	1.17
6.06	2.21	2.85	1.96	1.42	1.40	1.35
6.96	2.60	3.20	2.26	1.68	1.66	1.55
8.00	2.83	3.42	2.58	1.92	1.92	1.71
9.19	3.03	3.66	2.74	2.25	2.06	1.86
10.56	3.31	3.90	3.01	2.50	2.36	1.98
12.13	3.44	3.85	3.63	2.77	2.75	2.06
13.93	3.90	4.01	4.21	2.90	2.92	2.21
16.00	3.78	3.73	4.84	3.17	3.09	2.31
18.38	4.52	4.10	5.10	3.83	3.72	2.33
21.11	4.69	4.50	5.41	4.38	4.42	2.59
24.25	4.44	4.87	5.50	4.99	4.96	3.09
27.86	4.08	4.90	6.20	5.95	6.12	3.78
32.00	4.95	5.30	6.66	6.62	7.14	4.73
36.76	4.74	6.32	6.82	7.92	8.73	6.40
42.22	5.86	6.38	7.88	10.12	10.28	9.04
48.50	7.21	6.63	7.45	10.87	10.23	11.47
55.72	5.83	3.40	5.79	9.05	7.50	12.07
64.00	6.67	2.34	2.71	4.97	5.08	9.58
73.52	4.18	0.89	1.98	2.15	2.63	5.58
84.45				1.20	4.19	2.65
97.01						0.82
111.43						
128.00						

Station ID	T40B	T40B	T40B	T40B	T40B	T40 Avg
Stress	0.08	0.16	0.24	0.32	0.40	Bot Sed
Date	Feb-05	Feb-05	Feb-05	Feb-05	Feb-05	Feb-05
Diameter (um)						
0.76	1.56	1.15	0.73	1.11	0.82	0.47
0.87	1.72	1.22	0.80	1.17	0.84	0.51
1.00	1.81	1.33	0.91	1.29	0.89	0.56
1.15	1.79	1.41	0.97	1.43	0.94	0.60
1.32	1.84	1.55	1.07	1.58	1.00	0.65
1.52	1.89	1.59	1.17	1.73	1.02	0.71
1.74	1.94	1.71	1.23	1.73	1.07	0.79
2.00	2.15	1.79	1.31	1.78	1.18	0.85
2.30	2.11	1.91	1.41	1.83	1.21	0.94
2.64	2.25	2.01	1.59	1.73	1.31	1.03
3.03	2.54	2.03	1.73	1.70	1.44	1.11
3.48	2.63	2.37	1.82	1.76	1.56	1.26
4.00	3.09	2.78	2.02	1.82	1.65	1.41
4.59	2.90	2.90	2.19	2.02	1.69	1.38
5.28	3.29	3.32	2.45	2.10	1.96	1.61
6.06	3.63	3.81	2.83	2.44	2.26	1.87
6.96	4.16	4.40	3.29	2.77	2.59	2.11
8.00	4.61	4.80	3.61	3.09	2.93	2.38
9.19	4.98	5.10	3.96	3.26	3.33	2.65
10.56	5.12	5.33	4.17	3.61	3.63	2.81
12.13	5.03	5.28	4.28	3.78	3.95	2.94
13.93	4.94	5.05	4.51	3.90	4.28	3.12
16.00	4.61	4.95	4.50	4.05	4.49	3.33
18.38	4.62	4.57	4.78	4.16	4.61	3.54
21.11	4.44	4.32	5.05	4.29	4.76	3.84
24.25	3.58	3.76	5.44	4.44	4.99	4.17
27.86	3.42	3.52	5.35	4.82	4.98	4.59
32.00	2.85	3.26	5.41	4.65	5.20	5.40
36.76	3.35	2.93	5.20	5.19	5.27	6.43
42.22	2.02	3.11	4.97	5.30	5.85	7.73
48.50	2.42	2.90	4.29	5.09	6.17	9.10
55.72	2.73	2.20	3.84	4.60	5.09	8.65
64.00		1.66	3.10	3.64	4.37	6.97
73.52				2.15	1.74	3.58
84.45					0.90	0.90
97.01						
111.43						
128.00						

Station ID	T40G	T40G	T40G	T40G	T40G	T40 Avg
Stress	0.08	0.16	0.24	0.32	0.40	Bot Sed
Date	Feb-05	Feb-05	Feb-05	Feb-05	Feb-05	Feb-05
Diameter (um)						
0.76	1.43	1.35	1.53	1.15	1.30	0.47
0.87	1.54	1.49	1.67	1.27	1.43	0.51
1.00	1.76	1.57	1.74	1.34	1.44	0.56
1.15	1.91	1.62	1.72	1.40	1.42	0.60
1.32	2.06	1.71	1.76	1.49	1.47	0.65
1.52	2.21	1.82	1.84	1.57	1.57	0.71
1.74	2.32	1.93	1.92	1.68	1.58	0.79
2.00	2.47	2.05	2.05	1.75	1.69	0.85
2.30	2.50	2.05	2.06	1.84	1.81	0.94
2.64	2.63	2.27	2.28	1.98	1.88	1.03
3.03	3.00	2.66	2.55	2.06	1.98	1.11
3.48	2.87	2.73	2.62	2.20	2.01	1.26
4.00	3.09	2.84	2.70	2.45	2.30	1.41
4.59	3.42	3.22	2.95	2.49	2.43	1.38
5.28	3.73	3.55	3.31	2.70	2.48	1.61
6.06	4.10	4.01	3.85	3.33	3.05	1.87
6.96	4.44	4.47	4.25	3.78	3.46	2.11
8.00	4.60	5.01	4.91	4.17	3.87	2.38
9.19	4.82	5.27	5.37	4.58	4.27	2.65
10.56	4.37	5.38	5.49	4.90	4.51	2.81
12.13	4.60	5.48	5.61	5.06	4.77	2.94
13.93	3.88	5.52	5.42	5.30	4.60	3.12
16.00	3.36	5.20	5.23	5.20	4.84	3.33
18.38	3.46	4.46	4.71	5.12	4.68	3.54
21.11	3.31	4.07	4.73	4.86	4.82	3.84
24.25	2.95	3.70	4.30	4.76	4.80	4.17
27.86	2.78	3.72	4.46	4.29	4.59	4.59
32.00	2.49	3.37	3.42	3.62	4.43	5.40
36.76	2.07	3.16	2.93	3.48	4.62	6.43
42.22		2.28	2.62	3.36	4.14	7.73
48.50		2.03		3.46	3.71	9.10
55.72				1.48	2.04	8.65
64.00				1.89	1.54	6.97
73.52					0.47	3.58
84.45						0.90
97.01						
111.43						
128.00						

Station ID	T45D	T45D	T45D	T45D	T45D	T45 Avg
Stress	0.08	0.16	0.24	0.32	0.40	Bot Sed
Date	Feb-05	Feb-05	Feb-05	Feb-05	Feb-05	Feb-05
Diameter (um)						
0.76	1.66	1.40	1.36	1.29	1.22	0.77
0.87	1.66	1.38	1.48	1.30	1.25	0.83
1.00	1.73	1.43	1.55	1.30	1.22	0.87
1.15	1.87	1.54	1.68	1.36	1.25	0.93
1.32	2.05	1.68	1.80	1.46	1.30	1.01
1.52	2.20	1.75	1.82	1.57	1.35	1.07
1.74	2.51	1.85	1.97	1.72	1.42	1.09
2.00	2.49	2.00	2.03	1.89	1.41	1.23
2.30	2.57	1.95	2.35	2.01	1.58	1.26
2.64	2.94	2.13	2.31	2.10	1.63	1.39
3.03	3.03	2.33	2.57	2.25	1.78	1.51
3.48	3.22	2.63	2.68	2.17	1.85	1.52
4.00	3.72	2.67	2.67	2.59	2.07	1.74
4.59	3.74	3.03	3.21	2.93	2.25	1.99
5.28	4.18	3.50	3.52	3.35	2.60	2.27
6.06	4.69	4.05	4.00	3.92	3.15	2.53
6.96	5.21	4.77	4.54	4.60	3.66	2.83
8.00	5.55	5.31	4.98	5.20	4.14	3.03
9.19	5.91	5.66	5.41	5.52	4.65	3.22
10.56	6.10	5.74	5.66	6.12	5.06	3.28
12.13	6.02	5.79	5.62	5.81	5.44	3.38
13.93	5.60	5.48	5.61	6.15	5.59	3.29
16.00	4.57	5.57	5.26	5.74	5.43	3.33
18.38	4.54	4.76	4.75	5.61	5.39	3.31
21.11	4.39	4.61	4.61	4.92	5.31	3.69
24.25	3.22	3.94	4.03	4.23	5.03	4.31
27.86	2.57	3.16	2.97	2.94	4.87	4.84
32.00	2.05	2.76	3.47	3.02	4.07	5.73
36.76		2.40	2.51	3.76	4.05	6.84
42.22		1.72	2.22	1.62	3.40	7.67
48.50		1.17	1.33	1.56	2.55	7.73
55.72		1.01			1.83	5.79
64.00		0.81			1.28	4.06
73.52					0.91	1.15
84.45						
97.01						
111.43						
128.00						

Station ID	T45B	T45B	T45B	T45B	T45B	T45 Avg
Stress	0.08	0.16	0.24	0.32	0.40	Bot Sed
Date	Feb-05	Feb-05	Feb-05	Feb-05	Feb-05	Feb-05
Diameter (um)						
0.76	1.19	1.36	1.24	1.05	0.82	0.77
0.87	1.39	1.51	1.33	1.15	0.89	0.83
1.00	1.57	1.72	1.41	1.34	0.95	0.87
1.15	1.67	1.94	1.50	1.51	1.02	0.93
1.32	1.74	2.27	1.62	1.71	1.09	1.01
1.52	1.87	2.59	1.65	1.90	1.13	1.07
1.74	1.91	2.91	1.75	2.11	1.21	1.09
2.00	2.06	3.20	1.78	2.32	1.24	1.23
2.30	2.19	3.52	1.92	2.49	1.31	1.26
2.64	2.41	3.63	2.05	2.72	1.34	1.39
3.03	2.37	3.74	2.18	2.73	1.46	1.51
3.48	2.60	3.98	2.34	2.79	1.65	1.52
4.00	2.84	3.81	2.31	2.86	1.67	1.74
4.59	3.21	4.03	2.49	2.85	1.83	1.99
5.28	3.69	3.49	2.94	2.93	2.19	2.27
6.06	4.16	3.98	3.44	3.28	2.61	2.53
6.96	4.69	4.17	3.97	3.73	3.00	2.83
8.00	4.93	4.42	4.33	3.99	3.55	3.03
9.19	5.24	4.49	4.62	4.37	3.84	3.22
10.56	5.14	4.50	4.74	4.42	4.22	3.28
12.13	5.25	4.11	4.81	4.51	4.40	3.38
13.93	5.40	3.42	4.83	4.40	4.63	3.29
16.00	5.06	3.24	4.61	4.37	5.04	3.33
18.38	4.66	3.37	4.66	4.12	5.16	3.31
21.11	4.28	3.00	4.40	4.04	5.58	3.69
24.25	4.01	2.68	4.21	3.84	5.68	4.31
27.86	3.30	2.57	4.07	3.66	5.70	4.84
32.00	2.59	2.07	3.53	3.47	5.16	5.73
36.76	2.38	2.19	3.72	3.54	5.10	6.84
42.22	2.74	2.28	3.28	3.19	4.49	7.67
48.50	2.02	2.09	3.67	3.12	4.43	7.73
55.72	1.45	2.22	2.57	2.41	3.74	5.79
64.00		1.52	2.06	1.85	2.64	4.06
73.52				1.28	1.20	1.15
84.45						
97.01						
111.43						
128.00						

Station ID	T56F	T56F	T56F	T56F	T56F	T56 Avg
Stress	0.08	0.16	0.24	0.32	0.40	Bot Sed
Date	Feb-05	Feb-05	Feb-05	Feb-05	Feb-05	Feb-05
Diameter (um)						
0.76	1.05	1.47	1.42	1.54	1.02	0.90
0.87	1.12	1.48	1.47	1.56	1.07	0.93
1.00	1.20	1.55	1.54	1.60	1.18	1.01
1.15	1.33	1.63	1.59	1.68	1.32	1.06
1.32	1.53	1.77	1.73	1.70	1.49	1.14
1.52	1.71	1.92	1.80	1.75	1.67	1.20
1.74	1.90	2.11	1.85	1.72	1.87	1.28
2.00	1.97	2.11	1.96	1.74	2.03	1.29
2.30	2.12	2.21	2.07	1.67	2.20	1.42
2.64	2.20	2.30	2.13	1.85	2.27	1.48
3.03	2.39	2.38	1.98	1.98	2.32	1.67
3.48	2.61	2.42	2.29	2.09	2.51	1.75
4.00	3.10	2.83	2.52	2.41	2.43	1.98
4.59	3.20	2.77	2.78	2.37	2.48	2.08
5.28	3.55	3.06	3.13	2.73	2.72	2.37
6.06	4.03	3.55	3.66	3.19	3.13	2.80
6.96	4.66	4.37	4.21	3.70	3.49	3.34
8.00	5.40	4.53	4.84	4.26	3.90	3.77
9.19	5.77	5.00	5.39	4.81	4.42	4.30
10.56	6.14	5.35	5.89	5.33	4.87	4.72
12.13	6.43	5.61	6.37	5.94	5.49	5.25
13.93	6.25	5.94	6.27	6.10	5.95	5.41
16.00	5.64	5.49	6.11	5.91	6.09	5.55
18.38	5.50	5.39	5.29	5.93	6.09	5.81
21.11	5.29	5.01	5.71	5.29	5.78	5.57
24.25	4.33	4.51	4.78	5.13	5.30	5.24
27.86	3.90	3.90	3.94	4.54	4.55	5.13
32.00	3.26	3.40	2.90	3.98	4.20	4.60
36.76	2.14	2.87	1.91	2.98	3.76	4.58
42.22	0.26	1.68	1.81	2.77	2.47	4.08
48.50		0.78	0.67	1.77	1.93	3.73
55.72		0.64				2.71
64.00						1.82
73.52						
84.45						
97.01						
111.43						
128.00						

Station ID	T56A		T56A	T56A	T56A	T56 Avg
Stress	0.08		0.24	0.32	0.40	Bot Sed
Date	Feb-05		Feb-05	Feb-05	Feb-05	Feb-05
Diameter (um)						
0.76	1.00		0.92	0.92	1.12	0.90
0.87	1.15		1.02	0.99	1.24	0.93
1.00	1.28		1.17	1.09	1.36	1.01
1.15	1.44		1.25	1.18	1.37	1.06
1.32	1.59		1.39	1.29	1.47	1.14
1.52	1.68		1.55	1.43	1.54	1.20
1.74	1.72		1.73	1.54	1.55	1.28
2.00	1.89		1.89	1.71	1.69	1.29
2.30	1.86		1.97	1.79	1.80	1.42
2.64	2.27		2.13	1.79	1.93	1.48
3.03	2.40		2.16	1.93	2.08	1.67
3.48	2.87		2.36	1.93	2.25	1.75
4.00	2.81		2.51	2.23	2.51	1.98
4.59	3.35		2.83	2.12	2.77	2.08
5.28	3.77		3.20	2.42	3.17	2.37
6.06	4.30		3.75	2.77	3.77	2.80
6.96	4.96		4.26	3.19	4.24	3.34
8.00	5.55		4.65	3.52	4.88	3.77
9.19	5.74		5.14	3.93	5.75	4.30
10.56	5.53		5.67	4.34	5.85	4.72
12.13	4.96		5.72	4.80	6.46	5.25
13.93	4.48		5.73	4.91	6.36	5.41
16.00	3.75		5.49	5.55	6.33	5.55
18.38	2.33		4.92	5.43	6.22	5.81
21.11	2.00		4.61	5.77	5.90	5.57
24.25	1.68		4.27	5.91	4.87	5.24
27.86	1.15		4.06	5.74	4.80	5.13
32.00	0.91		3.41	5.19	2.74	4.60
36.76			3.51	4.67	2.72	4.58
42.22			2.41	3.95	1.28	4.08
48.50			1.82	2.69		3.73
55.72			1.35	1.54		2.71
64.00			0.37	1.74		1.82
73.52						
84.45						
97.01						
111.43						
128.00						

Station ID	T74H	T74H	T74H	T74H	T74H	T74 Avg
Stress	0.08	0.16	0.24	0.32	0.40	Bot Sed
Date	Feb-05	Feb-05	Feb-05	Feb-05	Feb-05	Feb-05
Diameter (um)						
0.76	1.44	1.41	1.24	1.34	1.12	0.95
0.87	1.45	1.45	1.30	1.41	1.22	0.98
1.00	1.46	1.50	1.42	1.50	1.32	1.04
1.15	1.54	1.57	1.54	1.61	1.45	1.12
1.32	1.69	1.72	1.64	1.70	1.55	1.19
1.52	1.79	1.87	1.76	1.83	1.68	1.27
1.74	1.92	1.96	1.85	1.88	1.80	1.32
2.00	2.13	2.00	1.91	1.99	1.83	1.40
2.30	2.43	2.01	2.08	2.01	2.01	1.47
2.64	2.53	2.25	2.23	2.33	2.15	1.58
3.03	2.70	2.38	2.34	2.43	2.26	1.69
3.48	2.83	2.29	2.80	2.77	2.35	1.86
4.00	2.89	3.02	2.90	3.14	2.46	2.08
4.59	2.83	2.71	2.80	2.86	2.58	2.37
5.28	3.11	3.20	3.29	3.41	3.10	2.74
6.06	3.43	3.61	3.81	4.06	3.69	3.20
6.96	3.77	3.93	4.50	4.71	4.26	3.75
8.00	3.91	4.56	5.13	5.10	4.92	4.26
9.19	3.82	4.65	5.63	5.63	5.40	4.74
10.56	3.79	5.20	6.24	6.21	5.83	5.25
12.13	3.74	5.12	6.45	6.39	6.14	5.55
13.93	3.11	4.87	6.43	6.53	6.42	5.85
16.00	2.21	4.83	6.39	6.37	6.23	5.80
18.38	2.67	4.62	5.78	5.47	6.33	5.83
21.11	2.47	4.00	5.42	4.80	5.69	5.60
24.25	2.47	3.18	4.39	3.90	4.69	5.39
27.86	2.25	2.87	3.33	3.27	3.75	4.94
32.00	1.95	1.39	2.77	2.36	2.66	4.45
36.76			1.51	1.75	2.03	4.01
42.22			1.14	1.24	1.59	3.22
48.50					0.64	2.20
55.72					0.45	1.60
64.00					0.43	0.96
73.52						0.34
84.45						
97.01						
111.43						
128.00						

Station ID	T74B	T74B	T74B	T74B	T74B	T74 Avg
Stress	0.08	0.16	0.24	0.32	0.40	Bot Sed
Date	Feb-05	Feb-05	Feb-05	Feb-05	Feb-05	Feb-05
Diameter (um)						
0.76	1.65	1.84		1.69	1.19	0.95
0.87	1.86	1.97	1.89	1.70	1.32	0.98
1.00	1.99	2.08	1.85	1.74	1.43	1.04
1.15	2.16	2.17	1.90	1.82	1.51	1.12
1.32	2.27	2.34	2.00	1.98	1.62	1.19
1.52	2.34	2.60	2.10	2.09	1.70	1.27
1.74	2.53	2.70	2.27	2.20	1.83	1.32
2.00	2.55	2.98	2.37	2.37	1.88	1.40
2.30	2.55	3.02	2.49	2.48	1.86	1.47
2.64	2.77	3.11	2.59	2.53	2.12	1.58
3.03	2.86	3.09	2.71	2.87	2.22	1.69
3.48	3.43	3.58	3.26	2.87	2.49	1.86
4.00	3.50	3.27	3.19	3.08	2.56	2.08
4.59	3.43	3.10	3.07	3.06	2.77	2.37
5.28	3.93	3.46	3.55	3.41	3.23	2.74
6.06	4.41	4.00	4.17	3.99	3.74	3.20
6.96	4.98	4.52	4.70	4.53	4.46	3.75
8.00	5.34	4.96	5.28	5.11	5.09	4.26
9.19	5.69	5.35	5.71	5.52	5.53	4.74
10.56	5.83	5.73	6.22	6.02	6.19	5.25
12.13	5.69	5.47	6.61	6.30	6.47	5.55
13.93	5.54	5.36	6.06	6.14	6.34	5.85
16.00	4.92	5.03	5.42	5.76	6.14	5.80
18.38	3.98	4.40	4.85	5.28	5.69	5.83
21.11	3.34	3.76	4.24	4.47	5.40	5.60
24.25	3.85	2.81	3.32	3.31	4.81	5.39
27.86	2.54	2.70	3.30	2.51	3.48	4.94
32.00	2.52	2.22	2.39	2.69	3.34	4.45
36.76	1.56	0.98	1.36	1.86	2.14	4.01
42.22		1.39	1.14	0.60	1.47	3.22
48.50						2.20
55.72						1.60
64.00						0.96
73.52						0.34
84.45						
97.01						
111.43						
128.00						

Station ID	T20H	T20H	T20H	T20H	T20H	T20 Avg
Stress	0.08	0.16	0.24	0.32	0.40	Bot Sed
Date	Apr-05	Apr-05	Apr-05	Apr-05	Apr-05	Apr-05
Diameter (um)						
0.76	0.83	1.17	0.64	0.50	0.33	0.23
0.87	0.87	1.25	0.71	0.58	0.37	0.27
1.00	0.93	1.35	0.79	0.65	0.40	0.30
1.15	0.95	1.38	0.87	0.72	0.44	0.36
1.32	1.04	1.32	0.95	0.79	0.49	0.40
1.52	1.12	1.36	1.06	0.89	0.50	0.47
1.74	1.17	1.41	1.17	1.00	0.55	0.54
2.00	1.27	1.33	1.27	1.12	0.59	0.60
2.30	1.40	1.42	1.38	1.14	0.67	0.71
2.64	1.44	1.46	1.52	1.34	0.66	0.78
3.03	1.61	1.54	1.67	1.53	0.77	0.94
3.48	1.84	1.54	1.87	1.47	0.86	1.11
4.00	1.85	1.63	2.23	1.74	0.92	1.30
4.59	2.05	1.68	2.41	1.89	1.18	1.44
5.28	2.31	2.02	2.79	2.24	1.03	1.68
6.06	2.56	2.22	3.24	2.66	1.26	2.04
6.96	2.81	2.39	3.61	3.10	1.48	2.42
8.00	2.95	2.52	4.07	3.48	1.73	2.82
9.19	2.90	2.73	4.37	4.03	2.01	3.29
10.56	3.16	3.49	4.71	4.26	2.28	3.69
12.13	2.87	4.39	4.71	4.75	2.63	4.21
13.93	3.00	4.71	4.78	5.10	2.94	4.68
16.00	3.44	5.48	5.27	5.41	3.33	4.97
18.38	3.35	5.41	4.99	5.21	3.81	5.26
21.11	3.52	5.52	5.03	5.23	4.14	5.58
24.25	3.69	5.47	5.14	5.46	4.56	5.80
27.86	3.48	4.48	4.62	5.27	5.22	5.84
32.00	4.20	4.22	4.34	5.19	5.51	6.36
36.76	4.96	4.73	4.17	5.01	5.66	6.18
42.22	5.74	4.32	3.84	4.57	6.25	6.00
48.50	6.11	5.13	3.66	4.55	7.43	5.88
55.72	6.76	4.05	3.21	4.14	8.19	4.96
64.00	4.57	4.20	2.45	3.31	7.46	4.72
73.52	5.65	2.67	1.44	1.67	6.63	2.61
84.45	3.61		0.99		4.00	1.59
97.01						
111.43						
128.00						

Station ID	T20B	T20B	T20B	T20B	T20B	T20 Avg
Stress	0.08	0.16	0.24	0.32	0.40	Bot Sed
Date	Apr-05	Apr-05	Apr-05	Apr-05	Apr-05	Apr-05
Diameter (um)						
0.76	0.32	0.13	0.51	0.36	0.26	0.23
0.87	0.37	0.15	0.60	0.41	0.30	0.27
1.00	0.39	0.17	0.68	0.47	0.34	0.30
1.15	0.42	0.18	0.78	0.52	0.39	0.36
1.32	0.44	0.20	0.87	0.59	0.45	0.40
1.52	0.47	0.22	0.98	0.64	0.50	0.47
1.74	0.53	0.24	1.08	0.72	0.53	0.54
2.00	0.61	0.25	1.19	0.80	0.59	0.60
2.30	0.59	0.29	1.37	0.90	0.67	0.71
2.64	0.67	0.31	1.41	1.02	0.75	0.78
3.03	0.79	0.33	1.69	1.08	0.84	0.94
3.48	0.72	0.40	1.73	1.26	0.94	1.11
4.00	0.97	0.42	2.18	1.45	1.19	1.30
4.59	0.90	0.43	2.03	1.56	1.26	1.44
5.28	0.84	0.48	2.28	1.95	1.32	1.68
6.06	0.97	0.61	2.71	1.94	1.56	2.04
6.96	1.02	0.68	3.09	2.24	1.85	2.42
8.00	1.10	0.74	3.57	2.61	2.12	2.82
9.19	1.13	0.71	3.77	2.96	2.44	3.29
10.56	1.25	0.91	4.05	3.31	2.74	3.69
12.13	1.31	1.07	4.00	3.66	3.64	4.21
13.93	1.31	1.30	4.33	4.15	4.35	4.68
16.00	1.43	1.50	4.18	4.30	4.50	4.97
18.38	1.78	1.73	4.44	4.87	5.10	5.26
21.11	1.91	1.96	4.62	5.01	5.24	5.58
24.25	2.24	2.31	4.64	4.73	5.58	5.80
27.86	3.06	3.18	4.14	5.01	6.18	5.84
32.00	3.87	4.28	4.57	5.31	6.42	6.36
36.76	5.80	6.44	4.49	5.79	6.79	6.18
42.22	9.05	9.77	4.69	5.42	6.35	6.00
48.50	12.54	13.91	4.64	5.83	6.43	5.88
55.72	15.40	15.94	4.70	6.48	7.41	4.96
64.00	12.49	16.28	4.59	5.32	5.55	4.72
73.52	8.63	9.49	3.68	4.25	3.04	2.61
84.45	4.66	2.98	1.73	3.08	2.39	1.59
97.01						
111.43						
128.00						

Station ID	T28B	T28B	T28B	T28B	T28B	T28 Avg
Stress	0.08	0.16	0.24	0.32	0.40	Bot Sed
Date	Apr-05	Apr-05	Apr-05	Apr-05	Apr-05	Apr-05
Diameter (um)						
0.76	0.67	1.09	0.32	0.36	0.34	0.36
0.87	0.72	1.11	0.36	0.39	0.37	0.39
1.00	0.79	1.17	0.40	0.43	0.39	0.44
1.15	0.79	1.17	0.42	0.47	0.42	0.46
1.32	0.88	1.30	0.49	0.51	0.45	0.50
1.52	0.94	1.34	0.51	0.56	0.50	0.55
1.74	0.91	1.41	0.55	0.59	0.53	0.59
2.00	1.04	1.36	0.59	0.67	0.57	0.66
2.30	1.04	1.56	0.62	0.70	0.62	0.70
2.64	1.13	1.65	0.69	0.75	0.62	0.78
3.03	1.36	2.05	0.80	0.87	0.74	0.85
3.48	1.48	1.97	0.88	0.97	0.82	0.96
4.00	1.47	2.11	1.03	0.99	0.88	1.02
4.59	1.79	2.22	1.05	1.16	0.96	1.05
5.28	2.05	2.57	1.25	1.37	1.00	1.30
6.06	2.45	2.86	1.46	1.58	1.22	1.43
6.96	2.76	3.00	1.67	1.84	1.40	1.65
8.00	3.28	3.19	1.88	2.08	1.66	1.80
9.19	3.75	3.24	2.08	2.30	1.84	2.08
10.56	4.22	3.20	2.23	2.51	2.09	2.27
12.13	4.51	3.35	2.45	2.78	2.39	2.43
13.93	5.44	3.86	2.61	3.09	2.63	2.68
16.00	6.14	4.31	2.68	3.02	3.07	2.75
18.38	6.03	4.37	2.84	3.30	3.70	3.07
21.11	6.82	4.22	3.27	3.83	4.18	3.35
24.25	7.04	4.98	3.53	4.16	4.72	3.57
27.86	6.57	5.05	4.49	4.73	5.08	4.00
32.00	6.27	4.47	5.19	5.42	6.17	4.52
36.76	5.08	5.47	6.40	6.57	7.07	5.54
42.22	4.21	5.52	8.64	7.79	8.33	7.50
48.50	3.11	5.11	12.03	8.95	10.27	10.13
55.72	1.80	5.91	12.31	9.73	9.91	11.92
64.00	1.40	3.81	8.72	8.68	9.11	10.63
73.52	2.07		4.09	3.76	3.65	5.84
84.45			1.47	2.17	2.34	1.89
97.01				0.93		0.34
111.43						
128.00						

Station ID	T28J	T28J	T28J	T28J	T28J	T28 Avg
Stress	0.08	0.16	0.24	0.32	0.40	Bot Sed
Date	Apr-05	Apr-05	Apr-05	Apr-05	Apr-05	Apr-05
Diameter (um)						
0.76	1.56	0.50	0.36	0.36		0.36
0.87	1.63	0.55	0.36	0.36		0.39
1.00	1.69	0.61	0.35	0.36	0.24	0.44
1.15	1.74	0.65	0.37	0.39	0.25	0.46
1.32	1.91	0.75	0.41	0.41	0.26	0.50
1.52	1.74	0.77	0.44	0.44	0.27	0.55
1.74	1.63	0.84	0.48	0.47	0.29	0.59
2.00	1.65	0.88	0.50	0.49	0.31	0.66
2.30	1.88	0.95	0.54	0.54	0.35	0.70
2.64	1.77	1.04	0.57	0.57	0.39	0.78
3.03	1.87	1.14	0.63	0.60	0.42	0.85
3.48	1.77	1.35	0.70	0.69	0.40	0.96
4.00	1.59	1.50	0.78	0.76	0.49	1.02
4.59	2.32	1.61	0.94	0.75	0.52	1.05
5.28	2.65	2.01	1.12	0.88	0.59	1.30
6.06	2.43	2.26	1.33	1.02	0.70	1.43
6.96	2.74	2.60	1.51	1.20	0.82	1.65
8.00	2.56	2.88	1.64	1.38	0.95	1.80
9.19	2.78	3.11	1.77	1.54	1.04	2.08
10.56	2.49	3.37	1.90	1.69	1.22	2.27
12.13	2.26	3.48	2.08	1.76	1.30	2.43
13.93	2.52	3.42	2.73	1.99	1.54	2.68
16.00	2.35	3.27	3.41	2.12	1.73	2.75
18.38	2.38	3.28	3.94	2.65	2.18	3.07
21.11	2.15	3.32	4.26	3.12	2.72	3.35
24.25	2.13	3.45	4.81	3.55	3.15	3.57
27.86	1.72	4.11	5.25	4.56	4.17	4.00
32.00	4.34	4.60	5.88	5.29	4.74	4.52
36.76	4.70	5.61	7.26	6.96	6.17	5.54
42.22	5.34	7.95	8.32	9.73	9.54	7.50
48.50	9.08	9.47	10.88	13.53	14.07	10.13
55.72	10.08	9.89	10.76	14.17	15.71	11.92
64.00	10.55	6.83	7.49	9.62	13.11	10.63
73.52		1.97	4.75	5.00	7.13	5.84
84.45			1.47	1.08	3.22	1.89
97.01						0.34
111.43						
128.00						

Station ID	T35B	T35B	T35B	T35B	T35B	T35 Avg
Stress	0.08	0.16	0.24	0.32	0.40	Bot Sed
Date	Apr-05	Apr-05	Apr-05	Apr-05	Apr-05	Apr-05
Diameter (um)						
0.76	1.35	0.71	0.93	0.63	0.39	0.30
0.87	1.45	0.84	1.03	0.71	0.43	0.32
1.00	1.53	0.94	1.16	0.79	0.47	0.35
1.15	1.67	1.00	1.25	0.86	0.50	0.36
1.32	1.80	1.12	1.32	0.91	0.52	0.38
1.52	1.91	1.24	1.45	0.98	0.57	0.41
1.74	2.05	1.30	1.52	1.03	0.58	0.44
2.00	2.17	1.41	1.65	1.05	0.61	0.47
2.30	2.32	1.55	1.72	1.24	0.64	0.51
2.64	2.51	1.70	1.81	1.20	0.72	0.55
3.03	2.54	1.82	2.14	1.56	0.80	0.62
3.48	2.81	2.19	2.46	1.54	0.80	0.67
4.00	3.27	2.34	2.58	1.66	0.95	0.66
4.59	3.40	2.60	2.88	2.02	1.03	0.76
5.28	3.47	3.12	3.44	2.21	1.24	0.85
6.06	3.90	3.71	4.02	2.65	1.49	0.99
6.96	4.48	4.23	4.64	3.07	1.75	1.13
8.00	4.94	4.70	5.15	3.40	2.02	1.28
9.19	5.38	5.25	5.48	3.72	2.40	1.41
10.56	5.10	5.52	5.58	3.96	2.65	1.51
12.13	5.54	5.53	5.53	4.04	2.87	1.73
13.93	5.73	5.40	5.39	4.13	3.03	1.80
16.00	5.36	5.09	4.99	4.26	3.30	1.91
18.38	5.57	4.99	4.79	4.31	3.57	2.31
21.11	5.28	4.77	4.59	4.61	4.16	2.69
24.25	4.29	4.89	4.36	5.01	4.53	3.12
27.86	5.39	4.55	4.27	5.11	5.11	3.83
32.00	2.65	4.52	4.07	5.22	6.29	4.69
36.76	2.11	4.11	3.40	5.82	7.56	6.22
42.22		3.25	3.27	5.72	9.21	8.24
48.50		2.35	1.91	6.67	10.82	10.70
55.72		1.63	1.23	4.15	9.47	12.73
64.00		1.65		3.43	5.64	12.47
73.52				2.35	2.52	8.57
84.45					1.35	4.06
97.01						0.96
111.43						
128.00						

Station ID	T35H	T35H	T35H	T35H	T35H	T35 Avg
Stress	0.08	0.16	0.24	0.32	0.40	Bot Sed
Date	Apr-05	Apr-05	Apr-05	Apr-05	Apr-05	Apr-05
Diameter (um)						
0.76	0.54	0.65			0.36	0.30
0.87	0.53	0.65	0.65	0.49	0.36	0.32
1.00	0.54	0.66	0.64	0.48	0.38	0.35
1.15	0.56	0.72	0.67	0.52	0.39	0.36
1.32	0.62	0.82	0.75	0.57	0.43	0.38
1.52	0.64	0.86	0.79	0.59	0.47	0.41
1.74	0.69	0.97	0.88	0.66	0.51	0.44
2.00	0.75	1.00	0.96	0.69	0.56	0.47
2.30	0.82	1.08	0.94	0.73	0.55	0.51
2.64	0.83	1.22	0.98	0.75	0.62	0.55
3.03	0.92	1.30	1.12	0.79	0.61	0.62
3.48	0.94	1.53	1.43	0.83	0.65	0.67
4.00	1.03	1.63	1.56	1.04	0.71	0.66
4.59	1.14	1.76	1.55	1.09	0.79	0.76
5.28	1.25	2.05	1.77	1.21	0.83	0.85
6.06	1.37	2.42	2.05	1.37	1.00	0.99
6.96	1.48	2.80	2.39	1.66	1.16	1.13
8.00	1.67	3.16	2.78	1.85	1.36	1.28
9.19	1.76	3.42	3.01	2.08	1.57	1.41
10.56	1.88	3.77	3.25	2.30	1.70	1.51
12.13	1.88	3.88	3.41	2.46	2.08	1.73
13.93	1.99	3.88	3.58	2.64	2.43	1.80
16.00	2.02	4.02	3.62	2.85	2.96	1.91
18.38	2.21	4.09	3.79	3.21	3.11	2.31
21.11	2.25	4.30	4.09	3.71	3.63	2.69
24.25	2.50	4.57	4.31	4.02	3.97	3.12
27.86	2.51	4.89	5.25	4.84	4.45	3.83
32.00	3.13	5.20	5.61	5.68	6.06	4.69
36.76	4.53	6.20	6.47	7.17	7.19	6.22
42.22	6.62	6.39	7.51	9.71	10.06	8.24
48.50	10.75	7.19	8.61	11.33	12.17	10.70
55.72	14.18	5.99	7.88	10.96	11.84	12.73
64.00	13.42	4.15	4.49	7.38	8.92	12.47
73.52	7.46	1.98	2.09	3.27	5.01	8.57
84.45	3.54	0.79	1.15	1.06	1.13	4.06
97.01	1.07					0.96
111.43						
128.00						

Station ID	T40H	T40H	T40H	T40H	T40H	T40 Avg
Stress	0.08	0.16	0.24	0.32	0.40	Bot Sed
Date	Apr-05	Apr-05	Apr-05	Apr-05	Apr-05	Apr-05
Diameter (um)						
0.76	1.21	0.53	0.68	0.59	0.70	0.57
0.87	1.25	0.59	0.75	0.66	0.75	0.61
1.00	1.27	0.66	0.82	0.74	0.84	0.65
1.15	1.37	0.70	0.93	0.83	0.90	0.71
1.32	1.40	0.77	0.99	0.90	0.99	0.77
1.52	1.46	0.82	1.03	0.95	1.04	0.80
1.74	1.64	0.88	1.12	0.98	1.14	0.83
2.00	1.62	0.97	1.21	1.05	1.13	0.88
2.30	1.80	1.00	1.24	1.16	1.33	0.96
2.64	1.76	1.11	1.35	1.21	1.44	1.01
3.03	2.01	1.22	1.49	1.42	1.43	1.11
3.48	2.19	1.27	1.50	1.54	1.66	1.10
4.00	1.98	1.43	1.73	1.66	1.63	1.36
4.59	1.94	1.68	2.15	1.91	2.05	1.40
5.28	2.06	2.00	2.33	1.99	1.82	1.65
6.06	2.31	2.39	2.80	2.32	2.10	1.90
6.96	2.52	2.79	3.13	2.70	2.41	2.00
8.00	2.57	3.23	3.50	3.02	2.72	2.19
9.19	2.75	3.57	3.75	3.30	2.94	2.41
10.56	2.60	3.94	4.06	3.64	3.30	2.61
12.13	2.79	4.30	4.16	3.85	3.31	2.80
13.93	2.77	4.19	4.33	3.81	3.44	2.98
16.00	3.26	4.44	4.53	3.67	3.73	3.17
18.38	3.22	4.68	3.99	3.61	4.26	3.36
21.11	2.95	4.94	3.88	4.02	4.56	3.83
24.25	2.89	5.12	3.75	4.27	4.64	4.28
27.86	2.78	5.36	4.31	4.50	5.13	4.94
32.00	3.10	5.50	4.91	4.81	5.21	5.94
36.76	4.15	6.55	5.10	5.85	5.86	7.14
42.22	5.66	6.23	5.65	7.40	6.18	8.02
48.50	6.88	6.40	6.04	7.05	7.05	8.91
55.72	6.40	5.08	5.86	6.89	7.08	8.20
64.00	7.56	3.61	4.57	4.64	4.75	6.05
73.52	5.77	2.04	2.37	3.06	2.48	3.23
84.45	2.11					1.64
97.01						
111.43						
128.00						

Station ID	T40C	T40C	T40C	T40C	T40C	T40 Avg
Stress	0.08	0.16	0.24	0.32	0.40	Bot Sed
Date	Apr-05	Apr-05	Apr-05	Apr-05	Apr-05	Apr-05
Diameter (um)						
0.76	1.16	1.26	0.84	0.94	0.83	0.57
0.87	1.24	1.37	0.92	0.97	0.92	0.61
1.00	1.30	1.46	0.99	1.05	1.05	0.65
1.15	1.42	1.51	1.07	1.13	1.21	0.71
1.32	1.50	1.64	1.18	1.28	1.40	0.77
1.52	1.56	1.75	1.23	1.41	1.59	0.80
1.74	1.67	1.90	1.35	1.53	1.65	0.83
2.00	1.84	1.98	1.43	1.70	1.74	0.88
2.30	1.93	2.02	1.53	1.78	1.69	0.96
2.64	2.02	2.22	1.62	1.96	1.69	1.01
3.03	2.20	2.28	1.79	2.07	1.45	1.11
3.48	2.31	2.59	2.02	2.03	1.52	1.10
4.00	2.45	2.68	2.18	2.04	1.62	1.36
4.59	2.75	3.26	2.47	2.12	1.85	1.40
5.28	2.98	3.24	2.95	2.37	2.16	1.65
6.06	3.35	3.74	3.49	2.76	2.52	1.90
6.96	3.83	4.09	4.01	3.02	2.86	2.00
8.00	4.42	4.40	4.36	3.29	3.29	2.19
9.19	5.09	4.92	4.67	3.45	3.55	2.41
10.56	5.62	4.64	4.68	3.68	3.91	2.61
12.13	6.30	4.63	4.68	3.73	4.15	2.80
13.93	6.80	4.65	4.71	3.68	4.30	2.98
16.00	6.75	4.29	4.61	3.46	4.43	3.17
18.38	6.90	4.14	4.69	3.48	4.36	3.36
21.11	6.02	4.31	4.56	3.55	4.65	3.83
24.25	5.42	4.40	4.48	3.76	4.93	4.28
27.86	4.13	3.47	4.57	4.18	5.02	4.94
32.00	2.58	3.63	4.03	4.36	5.15	5.94
36.76	2.48	3.61	4.28	4.80	5.67	7.14
42.22	1.99	3.21	4.12	4.96	5.40	8.02
48.50		2.98	4.18	6.08	5.22	8.91
55.72		2.48	3.48	5.27	4.10	8.20
64.00		1.24	2.01	4.85	2.93	6.05
73.52			0.84	2.23	1.20	3.23
84.45				1.03		1.64
97.01						
111.43						
128.00						

Station ID	T45I	T45I	T45I	T45I	T45I	T45 Avg
Stress	0.08	0.16	0.24	0.32	0.40	Bot Sed
Date	Apr-05	Apr-05	Apr-05	Apr-05	Apr-05	Apr-05
Diameter (um)						
0.76	1.47	1.17	1.03	1.00	1.00	0.79
0.87	1.67	1.28	1.12	1.09	1.07	0.84
1.00	1.75	1.37	1.20	1.16	1.16	0.92
1.15	1.78	1.47	1.32	1.26	1.25	1.00
1.32	1.94	1.56	1.41	1.37	1.39	1.07
1.52	2.01	1.67	1.51	1.56	1.51	1.14
1.74	2.11	1.71	1.64	1.67	1.58	1.21
2.00	2.11	1.92	1.72	1.69	1.71	1.32
2.30	2.60	2.00	1.80	1.88	1.79	1.41
2.64	2.26	2.18	1.92	2.00	2.05	1.45
3.03	2.76	2.35	1.97	2.22	2.17	1.62
3.48	3.01	2.46	2.15	2.41	2.39	1.77
4.00	2.84	2.94	2.35	2.28	2.65	2.12
4.59	3.23	3.28	2.73	2.73	2.93	2.14
5.28	3.73	3.81	3.18	3.22	3.44	2.40
6.06	4.28	4.33	3.76	3.77	4.05	2.60
6.96	4.51	5.10	4.39	4.24	4.60	2.69
8.00	4.89	5.42	4.82	4.73	5.19	3.00
9.19	5.08	5.78	5.18	5.05	5.60	3.22
10.56	5.24	5.77	5.49	5.30	5.84	3.52
12.13	5.50	6.02	5.33	5.62	5.99	3.73
13.93	5.08	5.43	5.42	5.69	6.15	3.95
16.00	5.40	5.25	5.39	5.43	5.49	4.02
18.38	5.36	4.92	5.63	5.26	5.82	4.45
21.11	4.89	4.39	4.99	4.95	5.24	4.52
24.25	4.18	3.96	4.94	4.82	5.12	4.72
27.86	3.60	3.03	4.65	4.24	4.18	4.45
32.00	2.33	3.10	3.29	3.69	3.47	4.57
36.76	1.31	2.08	3.24	2.70	2.24	4.68
42.22	0.59	1.59	2.44	2.67	1.46	5.05
48.50	1.28	1.82	2.67	2.50	0.96	5.43
55.72	1.24	0.84	1.33	0.96	0.53	5.07
64.00				0.86		4.35
73.52						3.57
84.45						1.23
97.01						
111.43						
128.00						

Station ID	T45B	T45B	T45B	T45B	T45B	T45 Avg
Stress	0.08	0.16	0.24	0.32	0.40	Bot Sed
Date	Apr-05	Apr-05	Apr-05	Apr-05	Apr-05	Apr-05
Diameter (um)						
0.76	1.51	0.65	0.86	0.97	0.91	0.79
0.87	1.56	0.71	0.95	1.04	0.99	0.84
1.00	1.70	0.80	1.04	1.16	1.10	0.92
1.15	1.76	0.86	1.16	1.25	1.19	1.00
1.32	1.91	0.98	1.27	1.35	1.32	1.07
1.52	1.94	1.01	1.34	1.36	1.35	1.14
1.74	2.29	1.09	1.41	1.56	1.49	1.21
2.00	2.19	1.24	1.46	1.64	1.58	1.32
2.30	2.31	1.34	1.69	1.75	1.64	1.41
2.64	2.42	1.42	1.68	1.90	1.77	1.45
3.03	2.38	1.48	1.80	1.98	2.15	1.62
3.48	2.76	1.60	1.91	2.33	2.29	1.77
4.00	2.98	1.94	2.06	2.31	2.38	2.12
4.59	3.12	2.23	2.63	2.70	2.63	2.14
5.28	3.60	2.58	2.81	3.19	3.04	2.40
6.06	3.94	2.92	3.25	3.69	3.45	2.60
6.96	4.50	3.34	3.77	4.35	3.93	2.69
8.00	4.82	3.75	4.10	4.70	4.24	3.00
9.19	5.22	3.91	4.66	4.99	4.82	3.22
10.56	5.42	4.15	4.93	5.41	4.90	3.52
12.13	5.70	4.79	5.09	5.18	4.83	3.73
13.93	5.33	4.42	5.08	5.45	4.94	3.95
16.00	5.35	5.48	4.99	5.38	4.54	4.02
18.38	4.81	5.91	5.07	4.62	4.43	4.45
21.11	3.50	5.88	5.06	4.57	4.24	4.52
24.25	4.06	6.01	4.96	4.37	4.19	4.72
27.86	3.72	5.44	4.38	3.92	4.26	4.45
32.00	5.04	5.14	4.05	3.58	4.13	4.57
36.76	4.17	4.68	4.07	3.13	4.09	4.68
42.22		4.41	3.70	3.24	3.95	5.05
48.50		3.44	3.32	3.04	3.61	5.43
55.72		3.26	2.64	2.43	2.29	5.07
64.00		2.16	1.52	1.49	2.05	4.35
73.52		0.98	0.84		1.27	3.57
84.45			0.46			1.23
97.01						
111.43						
128.00						

Station ID	T56X	T56X	T56X	T56X	T56X	T56 Avg
Stress	0.08	0.16	0.24	0.32	0.40	Bot sed
Date	Apr-05	Apr-05	Apr-05	Apr-05	Apr-05	Apr-05
Diameter (um)						
0.76	1.83	1.14	1.43	1.27	1.31	0.84
0.87	1.94	1.26	1.47	1.36	1.38	0.92
1.00	2.05	1.37	1.58	1.50	1.50	0.97
1.15	2.16	1.44	1.64	1.57	1.66	1.01
1.32	2.30	1.58	1.72	1.66	1.83	1.07
1.52	2.36	1.64	1.74	1.70	1.98	1.13
1.74	2.53	1.73	1.91	1.84	2.10	1.18
2.00	2.65	1.78	1.97	1.94	2.18	1.23
2.30	2.81	1.89	2.02	1.87	2.16	1.32
2.64	2.99	2.02	2.17	2.05	2.13	1.47
3.03	3.07	2.10	2.22	2.13	2.09	1.49
3.48	3.37	2.28	2.52	2.35	2.24	1.69
4.00	3.44	2.52	2.97	2.52	2.39	1.82
4.59	4.07	2.85	2.78	2.60	2.45	2.07
5.28	4.24	3.30	3.24	3.01	2.77	2.36
6.06	4.81	3.80	3.71	3.48	3.26	2.77
6.96	5.39	4.48	4.42	4.15	3.72	3.19
8.00	5.87	5.04	4.96	4.77	4.32	3.66
9.19	6.12	5.46	5.64	5.32	4.93	4.16
10.56	6.34	5.97	5.86	5.72	5.17	4.52
12.13	6.48	6.12	6.20	6.30	5.85	4.94
13.93	5.89	6.15	6.35	6.31	5.89	5.24
16.00	5.32	6.04	6.01	6.10	5.95	5.41
18.38	4.39	5.50	5.88	6.36	5.40	5.48
21.11	3.69	4.99	5.30	5.49	5.07	5.87
24.25	2.55	5.01	4.39	4.74	4.73	5.95
27.86	0.91	3.93	3.78	4.92	4.19	5.54
32.00	0.46	3.64	2.41	3.29	3.49	5.66
36.76		2.27	2.27	2.46	2.85	5.04
42.22		1.91	1.44	1.24	1.98	4.30
48.50		0.80			1.47	3.61
55.72					0.65	2.73
64.00					0.46	1.34
73.52						
84.45						
97.01						
111.43						
128.00						

Station ID	T56B	T56B	T56B	T56B	T56B	T56 Avg
Stress	0.08	0.16	0.24	0.32	0.40	Bot sed
Date	Apr-05	Apr-05	Apr-05	Apr-05	Apr-05	Apr-05
Diameter (um)						
0.76	2.43	1.44	1.24	1.34	1.04	0.84
0.87	2.48	1.51	1.29	1.37	1.09	0.92
1.00	2.55	1.56	1.35	1.45	1.17	0.97
1.15	2.64	1.59	1.43	1.53	1.25	1.01
1.32	2.73	1.70	1.49	1.61	1.33	1.07
1.52	2.78	1.80	1.59	1.67	1.39	1.13
1.74	2.86	1.85	1.65	1.80	1.49	1.18
2.00	2.91	1.98	1.73	1.86	1.52	1.23
2.30	3.05	2.08	1.79	2.02	1.60	1.32
2.64	3.28	2.24	1.93	2.19	1.76	1.47
3.03	3.22	2.55	2.14	2.23	1.86	1.49
3.48	3.37	2.72	2.38	2.54	1.92	1.69
4.00	3.21	2.93	2.48	2.65	1.93	1.82
4.59	3.74	3.20	2.88	2.91	2.09	2.07
5.28	4.06	3.72	3.47	3.48	2.53	2.36
6.06	4.48	4.39	3.97	4.17	3.09	2.77
6.96	4.90	4.93	4.76	4.74	3.68	3.19
8.00	4.98	5.47	5.42	5.40	4.31	3.66
9.19	5.02	5.94	5.98	5.92	4.78	4.16
10.56	5.03	6.27	6.37	6.19	5.49	4.52
12.13	5.22	5.88	6.58	6.36	6.01	4.94
13.93	4.45	5.91	6.59	5.96	6.47	5.24
16.00	4.59	5.29	6.37	5.97	6.70	5.41
18.38	3.61	4.83	5.51	5.06	6.71	5.48
21.11	3.05	4.85	5.52	4.56	6.42	5.87
24.25	2.38	3.47	4.65	4.47	6.05	5.95
27.86	1.97	2.87	3.65	3.45	4.89	5.54
32.00	2.27	2.57	2.83	2.68	4.03	5.66
36.76	1.71	1.93	1.66	2.94	3.29	5.04
42.22	1.05	1.14	1.31	1.47	2.40	4.30
48.50		1.41			1.70	3.61
55.72						2.73
64.00						1.34
73.52						
84.45						
97.01						
111.43						
128.00						

Station ID	T74K	T74K	T74K	T74K	T74K	T74 Avg
Stress	0.08	0.16	0.24	0.32	0.40	Bot Sed
Date	Apr-05	Apr-05	Apr-05	Apr-05	Apr-05	Apr-05
Diameter (um)						
0.76	1.32	1.46	1.23	1.08	1.18	1.18
0.87	1.48	1.52	1.29	1.12	1.25	1.25
1.00	1.71	1.67	1.38	1.19	1.36	1.33
1.15	1.81	1.70	1.49	1.29	1.46	1.39
1.32	2.03	1.87	1.55	1.35	1.57	1.44
1.52	2.09	1.89	1.63	1.43	1.73	1.51
1.74	2.32	2.03	1.75	1.51	1.80	1.64
2.00	2.37	2.26	1.81	1.60	1.96	1.70
2.30	2.70	2.11	1.92	1.67	2.13	1.84
2.64	2.66	2.23	1.95	1.92	2.21	1.83
3.03	3.14	2.46	2.27	2.03	2.33	2.08
3.48	3.19	2.59	2.23	2.24	2.16	2.11
4.00	3.15	2.50	2.56	2.40	2.61	2.25
4.59	3.49	3.14	2.90	2.56	2.37	2.55
5.28	4.02	3.54	3.36	2.52	2.84	2.73
6.06	4.54	4.09	3.88	2.94	3.31	3.36
6.96	4.76	4.86	4.51	3.40	3.66	3.88
8.00	5.05	5.39	5.11	3.97	4.13	4.38
9.19	5.42	5.90	5.73	4.48	4.46	4.84
10.56	5.72	6.18	6.22	5.10	4.94	5.33
12.13	4.87	6.43	6.51	5.58	5.31	5.50
13.93	5.72	5.89	6.82	5.95	5.88	5.65
16.00	5.31	5.99	6.69	5.96	5.52	6.01
18.38	4.43	5.51	5.76	6.23	5.57	5.55
21.11	5.11	5.28	5.39	6.28	5.31	5.47
24.25	4.96	3.17	4.13	5.71	4.95	4.81
27.86	4.73	3.05	3.78	5.46	4.63	4.34
32.00	1.92	2.37	2.72	4.71	4.08	3.73
36.76		2.93	2.11	4.52	3.12	3.33
42.22			1.30	2.25	2.42	2.53
48.50				1.55	1.81	1.93
55.72					1.08	1.40
64.00					0.46	1.09
73.52					0.42	
84.45						
97.01						
111.43						
128.00						

Station ID	T74A	T74A	T74A	T74A	T74A	T74 Avg
Stress	0.08	0.16	0.24	0.32	0.40	Bot Sed
Date	Apr-05	Apr-05	Apr-05	Apr-05	Apr-05	Apr-05
Diameter (um)						
0.76	2.13	1.29	1.11	1.08	1.07	1.18
0.87	2.27	1.41	1.20	1.14	1.13	1.25
1.00	2.49	1.57	1.36	1.23	1.24	1.33
1.15	2.65	1.68	1.44	1.30	1.32	1.39
1.32	2.85	1.83	1.61	1.39	1.41	1.44
1.52	2.98	1.87	1.65	1.50	1.50	1.51
1.74	3.17	2.02	1.73	1.60	1.59	1.64
2.00	3.15	2.18	1.97	1.74	1.66	1.70
2.30	3.17	2.37	2.15	1.81	1.75	1.84
2.64	3.26	2.29	2.23	1.84	1.86	1.83
3.03	3.16	2.72	2.45	2.10	2.04	2.08
3.48	3.29	2.60	2.31	2.33	2.16	2.11
4.00	3.68	3.27	2.75	2.40	2.35	2.25
4.59	3.55	3.51	3.25	2.78	2.68	2.55
5.28	3.80	4.08	3.90	3.16	3.13	2.73
6.06	4.19	4.79	4.49	3.76	3.75	3.36
6.96	4.52	5.45	5.16	4.33	4.35	3.88
8.00	4.65	6.07	5.99	4.97	5.02	4.38
9.19	4.65	6.50	6.36	5.62	5.60	4.84
10.56	4.38	6.39	6.85	6.08	6.26	5.33
12.13	4.49	6.51	7.28	6.57	6.63	5.50
13.93	4.29	6.02	6.96	6.57	6.52	5.65
16.00	3.70	5.73	6.45	6.73	6.60	6.01
18.38	3.49	5.13	4.92	6.00	6.29	5.55
21.11	3.12	4.60	4.92	5.88	5.84	5.47
24.25	2.50	3.05	4.08	5.17	4.71	4.81
27.86	2.27	2.68	2.69	4.31	3.91	4.34
32.00	1.82	2.42	1.49	3.22	3.14	3.73
36.76	1.21		1.23	2.08	2.65	3.33
42.22				1.29	1.84	2.53
48.50						1.93
55.72						1.40
64.00						1.09
73.52						
84.45						
97.01						
111.43						
128.00						